Baghdad Science Journal

Volume 22 | Issue 6 Article 20

6-20-2025

The Role of Fear and Predator Dependent Refuge on a Stage Structure Prey-Predator System

Ghaith Jassim Abdulsada
Department of Mathematics, College of Science, University of Baghdad, Baghdad, Iraq,
ghaith.jassem1703a@sc.uobaghdad.edu.iq

Hiba Abdullah Ibrahim
Department of Mathematics, College of Science, University of Baghdad, Baghdad, Iraq,
hiba.ibrahim@sc.uobaghdad.edu.iq

How to Cite this Article

Abdulsada, Ghaith Jassim and Ibrahim, Hiba Abdullah (2025) "The Role of Fear and Predator Dependent Refuge on a Stage Structure Prey-Predator System," *Baghdad Science Journal*: Vol. 22: Iss. 6, Article 20.
DOI: https://doi.org/10.21123/2411-7986.4970

BAGHDAD SCIENCE JOURNAL 2025;22(6):1960–1979

Scan the QR to view the full-text article on the journal website

RESEARCH ARTICLE

The Role of Fear and Predator Dependent Refuge on a Stage Structure Prey-Predator System

Ghaith Jassim Abdulsada, Hiba Abdullah Ibrahim *

Department of Mathematics, College of Science, University of Baghdad, Baghdad, Iraq

ABSTRACT

The present paper investigates the role of fear and predator dependent refuge in the prey-predator system. The system describes the interaction between prey and a stage structure of predator that incorporates Holling II functional response. The predator splits into two compartments immature (juvenile) and mature (adult). The mature predators can hunt and reproduce but this capability is not found in the immature predators, the immature depend on their parents. The growth rate of prey decreases due to the existence of mature predators. The existence, uniqueness, and boundedness of the solution of the system are investigated. Three equilibrium points of the system are determined. The local stability of the system is studied. The global stability of the axial equilibrium point is discussed using the appropriate Lyapunov function, while the basin of attraction of the positive equilibrium point is investigated. The persistence constraints of the system are established. The local and Hopf bifurcation analyses of the system are examined. Lastly, numerical simulations are given to ensure the theoretical results with the help of Matlab program (version R2018b). It is found that the effect of fear plays a substantial role in the dynamic of the system. On the other hand, the refuge's coefficient continuously affects the system. Furthermore, the variation of the refuge's coefficient by utilizing different initial points leads to a change in the behavior of the system from stable to unstable and conversely.

Keywords: Boundedness, Equilibrium points, Local bifurcation, Persistence constraints, Stability analysis

Introduction

Ecological systems play a conclusive role in the preservation of ecology. During the last few years, many ecologists have given important attention to understanding the prey-predator systems with their interactions in the environment. Through the classic models, the Lotka-Volterra model represented the first model to describe the interaction between predator and their prey, it was introduced separately by Lotka[1] and Volterra.[2] Later, many researchers modified the Lotka-Volterra model to study the dynamics of prey-predator models, see.[3–5]

Many biological factors affect the dynamical behavior of these models, like disease,[6–8] harvesting,[9,10] cannibalism,[11–13] Allee effect,[14,15] migration,[16,17] and many different factors. Also, the functional response is the main part of prey-predator models. Holling types functional responses are widespread in the literature, especially type-I, type-II, type-III, and type-IV.[18–20]

In ecology, many species have life stages that involve two stages: immature and mature and every stage has different behavior. Several studies of stage structure prey-predator models have been suggested.[21–23] Bahlool[21] studied a stage structure prey-predator model with hunting cooperation and anti-predator, and she obtained that the conversion rate and hunting cooperation rate persistently impact the system.

In the natural world, there were substantial studies of the effect of fear on the dynamic behavior of ecological models. In an ecosystem, the prey is affected by the presence of predators as direct, indirect, or

Received 6 March 2024; revised 24 June 2024; accepted 26 June 2024.
Available online 20 June 2025

* Corresponding author.
E-mail addresses: ghaith.jassem1703a@sc.uobaghdad.edu.iq (G. J. Abdulsada), hiba.ibrahim@sc.uobaghdad.edu.iq (H. A. Ibrahim).

https://doi.org/10.21123/2411-7986.4970

both.[24–26] The predator hunts and devour the prey, (the direct effect). The existence of predators prompts fear in the prey which leads to a decrease in the growth rate of prey, (the indirect effect). Therefore, the fear plays an important role in the environment. Therefore, the impact of fear must be taken into regard since there are cases when the existence of fear leads to forces prey to quit their habitat.[24] Ibrahim and Naji[25] suggested the effect of fear on a food chain model with the Beddington–DeAngelis functional response, they obtained that the presence of fear made a stabilizing effect on the system.

On the other hand, many scholars focused on the study of prey's refuge, which is a biological feature and a critical element influencing the dynamical behavior of suggested models. Due to the presence of predators, the prey flees and seeks refuge, which leads to a reduced chance of predation. These phenomena are a helpful preservative measure for prey. Several studies have proven that refuges have stabilizing[27] and destabilizing impacts.[28] In light of the foregoing, prey refuge represented one of the main areas in mathematical modeling, and many researchers have made substantial discoveries in this field.[29–31] Hague and Sarwardi[31] proposed a harvested prey-predator model with prey's refuge in both species, they observed that refuge plays a main role in the dynamics of the system.

In this paper, a stage structure prey-predator system with Holling type II is created by integrating predation fear and predator-dependent refuge. In the next section, a mathematical system is formulated, and then the existence and boundedness of the system's solution are investigated. The stability analysis (locally and globally) and persistent constraints of the suggested system are studied respectively. Local bifurcation near all possible equilibrium points is analyzed. Numerical simulations were carried out to ensure the obtained results. At last, the conclusions are discussed. The purpose of this paper is to study the role of fear and refuge dependent on predators in the proposed prey-predator model and illustrate their dynamic behavior. Also, Our study shows that system 1 is affected by not only the fear effect but also the predator-dependent refuge. Numerical simulations illustrated that the high level of fear has a destabilizing effect which leads to periodic attractors, whilst the high level of predator-dependent refuge has a bi-stable case.

Mathematical model

A mathematical model consisting of a stage structure prey-predator system is suggested, which contains the impact of fear and predator-dependent refuge. In the absence of the predation process, the prey $x(t)$ grows logistically. The predator split into two parts, immature $y(t)$ and mature $z(t)$, it is supposed that the immature predator cannot hunt or replicate, relying on their parents (mature), while part from it enlarges to become mature. Furthermore, both the immature and mature predators meet natural death, while the prey's growth rate reduces due to fear of predation by mature predators. In addition, this model contains refuges proportional to the interactions between the prey and predator population, where $\alpha \in [0, 1]$ represented the refuge rate of prey. Hence, the number of refuges is αxz, while $x(1-\alpha z)$ represents the prey population to be predated by the predator. According to these suppositions, the mathematical model of prey-predator with Holling II functional response can be represented by three differential equations:

$$\begin{aligned}
\frac{dx}{dt} &= \frac{rx}{1+mz}\left(1-\frac{x}{k}\right) - \frac{a(1-\alpha z)xz}{b+(1-\alpha z)x} = F_1(x,y,z),\\
\frac{dy}{dt} &= \frac{ea(1-\alpha z)xz}{b+(1-\alpha z)x} - \beta y - d_1 y = F_2(x,y,z),\\
\frac{dz}{dt} &= \beta y - d_2 z = F_3(x,y,z),
\end{aligned} \tag{1}$$

where $x(0) \geq 0$, $y(0) \geq 0$, and $z(0) \geq 0$. All the above parameters are positive and explained in Table 1.

Also, the flow chart of the suggested system is shown in Fig. 1.

Moreover, the solution of system 1 with initial values $(x(0), y(0), z(0))$ is uniformly bounded (U.B) shown in the next Theorem.

Theorem 1: *System 1 has U.B solutions.*

Table 1. Parameters explanation.

Parameters	Explanation
r	The essential growth rate of prey.
m	The prey's fear rate.
k	The carrying capacity of the prey is given by the environment.
a	The consumption rate by the predator.
α	The refuge rate of prey.
b	The half-saturation constant.
e	Conversion rate.
β	Grown-up rate from an immature predator to a mature predator.
d_1	The natural death of the immature predator.
d_2	The natural death of the mature predator.

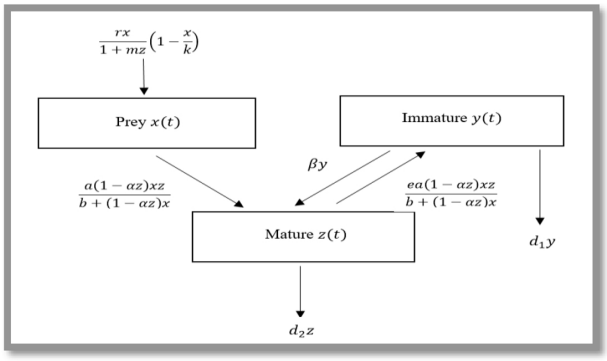

Fig. 1. Block diagram for system 1.

Proof: let $(x(t), y(t), z(t))$ be any solution of system 1, then from the 1st equation it is obtained that

$$\frac{dx}{dt} \le rx\left(1-\frac{x}{k}\right) \tag{2}$$

By applying a series of mathematical operations, it is obtained

$$x(t) \le \frac{kx_0}{x_0 + (k - x_0)\, e^{-rt}}.$$

Therefore, when $t \to \infty$, it is obtained that $x(t) \le k$.

Let $R(t) = x(t) + y(t) + z(t)$.

Now, by deriving $R(t)$ for time (t), and due to the meaning's biological of the parameters of system 1 and the bound of $x(t)$, then $\frac{dR}{dt} + LR \le B$, where $L = min\{\mu, d_1, d_2\}$, $B = k(r+\mu)$ and μ is a suitable positive constant.

By applying the Gronwall Lemma[32] of the above inequality, it is obtained

$$R(t) \le \frac{B}{L} + \left(R_0 - \frac{B}{L}\right) e^{-Lt},$$

Moreover, for $t \to \infty$, then $R(t) \le \frac{B}{L}$. Hence, all solutions of system 1 are U.B. □

Stability analysis of system 1

In this part, the existence of the equilibrium points (EP) of system 1 is investigated, and then their local stability is studied too. System 1 has three EP, as shown below.

The trivial equilibrium point (T.EP), is given by $\bar{x}_0 = (0, 0, 0)$ always exists.

The axial equilibrium point (A.EP), given by $\bar{x}_1 = (k, 0, 0)$ always exists.

The positive equilibrium point (P.EP), given by $\bar{x}_2 = (x^*, y^*, z^*)$, where

$$x^* = \frac{d_2 b\,(\beta + d_1)}{(1 - \alpha z^*)\,(\beta e a - d_2\,(\beta + d_1))}, \tag{3}$$

$$y^* = \frac{d_2}{\beta} z^*, \tag{4}$$

$$B_1(z)^4 + B_2(z)^3 + B_3(z)^2 + B_4 z + B_5 = 0, \tag{5}$$

Where

$$B_1 = -ak\alpha^2 m\left(\beta e a - d_2\,(\beta + d_1)\right)^2 < 0,$$

$$B_2 = -ak\alpha\,(\alpha - 2m)\left(\beta e a - d_2\,(\beta + d_1)\right)^2,$$

$$B_3 = ak\,(2\alpha - m)\left(\beta e a - d_2\,(\beta + d_1)\right)^2,$$

$$B_4 = -\,ak\left(\beta e a - d_2\,(\beta + d_1)\right)\left(\left(\beta e a - d_2\,(\beta + d_1)\right) + \alpha r b \beta e\right) < 0,$$

$$B_5 = rb\beta e a\left(k\left(\beta e a - d_2\,(\beta + d_1)\right) - d_2 b\,(\beta + d_1)\right).$$

There are different cases for P.EP $\bar{x}_2$. It is clear that the sign of the coefficients of the above polynomial depends on B_2, B_3, and B_5.

Now, by using Descartes' rule of signs,[33] the possibility of reaching the root of Eq. (5) has been discussed as illustrated below:

If $B_5 > 0$, there are three cases will be discussed,

Case I: In the range $\frac{m}{2} < \alpha < 2m$ leads to $B_2 > 0$, $B_3 > 0$, then the polynomial equation has either three or one positive root.

Case II: If $\alpha > 2m$ leads to $B_2\langle 0,\ B_3\rangle 0$, then the polynomial equation has either three or one positive root.

Case III: If $\alpha < \frac{m}{2}$ leads to $B_2 > 0$, $B_3 < 0$, then the polynomial equation has either three or one positive root.

According to the above cases, the P.EP exists in the $int.R_+^3$ if the following constraints are met:

$$d_2\,(\beta + d_1) < \beta e a \tag{6}$$

with one of the following sets of constraints.

$$\left.\begin{array}{l} B_2 > 0,\ B_3 > 0, B_5 > 0 \\ B_2 < 0,\ B_3 > 0, B_5 > 0 \\ B_2 > 0,\ B_3 < 0, B_5 > 0 \end{array}\right\} \tag{7}$$

Now, after finding all possible EP (biologically acceptable) of system 1, the linearization technique that depends on the Jacobian matrix (J.M) is used

to investigate the local stability of these points, followed by the calculated of the eigenvalues which describe the nature of these points. The J.M at T.EP is determined by

$$J(\bar{x}_0) = \begin{bmatrix} r & 0 & 0 \\ 0 & -(\beta + d_1) & 0 \\ 0 & \beta & -d_2 \end{bmatrix} \tag{8}$$

So, the eigenvalues of $J(\bar{x}_0)$ are $\lambda_{01} = r > 0,\ \lambda_{02} = -(\beta + d_1) < 0,\ \lambda_{03} = -d_2 < 0$. Thus $\bar{x}_0$ is a saddle point.

The J.M at A.EP is given by

$$J(\bar{x}_1) = \begin{bmatrix} -r & 0 & \frac{-ak}{b+k} \\ 0 & -(\beta + d_1) & \frac{eak}{b+k} \\ 0 & \beta & -d_2 \end{bmatrix} \tag{9}$$

Now, the characteristic equation of $J(\bar{x}_1)$ can be given as follows:

$$((-r) - \lambda)\left(\lambda^2 - T_1\lambda + D_1\right) = 0 \tag{10}$$

where

$$T_1 = -(\beta + d_1 + d_2) < 0,$$

$$D_1 = d_2(\beta + d_1) - \frac{\beta kea}{b+k}.$$

So, the eigenvalues of $J(\bar{x}_1)$ are $\lambda_{11} = -r < 0$, $\lambda_{12} = \frac{T_1}{2} + \frac{1}{2}\sqrt{{T_1}^2 - 4D_1}$, $\lambda_{13} = \frac{T_1}{2} - \frac{1}{2}\sqrt{{T_1}^2 - 4D_1}$.

It is clear that the two eigenvalues λ_{12} and λ_{13} that get from Eq. (10) have negative real parts and $\bar{x}_1$ is locally asymptotically stable (LAS) under the following constraint holds.

$$\frac{\beta kea}{b+k} < d_2(\beta + d_1) \tag{11}$$

The J.M at P.EP is determined by

$$J(\bar{x}_2) = \begin{bmatrix} a_{11} & 0 & a_{13} \\ a_{21} & a_{22} & a_{23} \\ 0 & a_{32} & a_{33} \end{bmatrix} \tag{12}$$

where

$$a_{11} = \left(\frac{r}{1+mz^*}\right)\left(1 - \frac{2x^*}{k}\right) - \frac{abz^*(1-\alpha z^*)}{\left(b + (1-\alpha z^*)x^*\right)^2},$$

$$a_{13} = -\left(\left(\frac{rmx^*}{(1+mz^*)^2}\right)\left(1 - \frac{x^*}{k}\right) + \frac{abx^*(1-2\alpha z^*) + a(x^*)^2(1-\alpha z^*)^2}{\left(b + (1-\alpha z^*)x^*\right)^2}\right),$$

$$a_{21} = \frac{eabz^*(1-\alpha z^*)}{\left(b + (1-\alpha z^*)x^*\right)^2},$$

$$a_{22} = -(\beta + d_1),$$

$$a_{23} = \frac{eabx^*(1-2\alpha z^*) + ea(x^*)^2(1-\alpha z^*)^2}{\left(b + (1-\alpha z^*)x^*\right)^2},$$

$$a_{32} = \beta,$$

$$a_{33} = -d_2.$$

Now, the characteristic equation of the $J(\bar{x}_2)$ of system 1 is given as follows

$$\lambda^3 + H_1\lambda^2 + H_2\lambda + H_3 = 0 \tag{13}$$

where

$$H_1 = -(a_{11} + a_{22} + a_{33})$$

$$H_2 = a_{11}a_{22} + a_{11}a_{33} + a_{22}a_{33} - a_{23}a_{32}$$

$$H_3 = a_{11}(a_{23}a_{32} - a_{22}a_{33}) - a_{13}a_{21}a_{32}$$

whilst,

$$\begin{aligned} \Delta = \ & H_1H_2 - H_3 \\ = & -a_{11}a_{22}(a_{11} + a_{22}) - a_{11}a_{33}(a_{11} + a_{33}) \\ & -(a_{22} + a_{33})(a_{22}a_{33} - a_{23}a_{32}) + W_1 + W_2. \end{aligned}$$

Here,

$$W_1 + W_2 = -2a_{11}a_{22}a_{33} + a_{13}a_{21}a_{32} \tag{14}$$

Applying the Routh-Hawirtiz Criterion,[34] the characteristic equation's roots 13 have negative real parts if the next constraints are met

$$H_1 > 0,\ H_3 > 0 \text{ and } \Delta = H_1H_2 - H_3 > 0.$$

Thus, Direct calculation detects that these constraints hold provided that

$$\frac{r}{1+mz^*} < \frac{2rx^*}{k(1+mz^*)} + \frac{abz^*(1-\alpha z^*)}{\left(b + (1-\alpha z^*)x^*\right)^2} \tag{15}$$

$$z^* < \frac{1}{2\alpha} \tag{16}$$

$$eax^*\left(b\left(1-2\alpha z^*\right)+x^*\left(1-\alpha z^*\right)^2\right) < d_2\left(\beta+d_1\right)\left(b+\left(1-\alpha z^*\right)x^*\right)^2 \quad (17)$$

$$\frac{2rd_2\left(\beta+d_1\right)}{\left(1+mz^*\right)}+\frac{\beta eabz^*\left(1-\alpha z^*\right)}{\left(b+\left(1-\alpha z^*\right)x^*\right)^2}\left(\left(\frac{rmx^*}{\left(1+mz^*\right)^2}\right)\times\left(1-\frac{x^*}{k}\right)+\frac{abx^*\left(1-2\alpha z^*\right)+a(x^*)^2(1-\alpha z^*)^2}{\left(b+\left(1-\alpha z^*\right)x^*\right)^2}\right) < 2d_2\left(\beta+d_1\right)\left(\frac{2rx^*}{k\left(1+mz^*\right)}+\frac{abz^*\left(1-\alpha z^*\right)}{\left(b+\left(1-\alpha z^*\right)x^*\right)^2}\right) \quad (18)$$

Then $\bar{x}_2$ is LAS under the above constraints 15–18.

Global stability of system 1

In this part, the global stability of system 1 is studied as shown in the next theorems, through applying suitable Lyapunov functions. The basin of attraction of trajectory to the dynamical system can be described as the state space or a particular region in it, depending on the state variables of the system.

Theorem 2: Suppose that the A.EP is LAS, then it is globally asymptotically stable (GAS) if the following constraint is met

$$\frac{ak}{b+k} < d_2 \quad (19)$$

Proof: Consider the following function

$$p_1(x,y,z)=\int_k^x\frac{u-k}{u}du+y+z \quad (20)$$

Obviously, the function p_1 is positive definite. So, $p_1(k,0,0)=0$ and $p_1(x,y,z)>0,\ \forall\ (x,y,z)\in R_+^3$ with $(x,y,z)\neq(k,0,0)$. Now, Eq. Eq. (20) is derived with respect to t, and then, using several simple computations, it's obtained

$$\frac{dp_1}{dt}=(x-k)\left(\frac{r}{1+mz}\left(1-\frac{x}{k}\right)-\frac{a\left(1-\alpha z\right)z}{b+\left(1-\alpha z\right)x}\right)+\left(\frac{ea\left(1-\alpha z\right)xz}{b+\left(1-\alpha z\right)x}-\beta y-d_1y\right)+\left(\beta y-d_2z\right),$$

$$\frac{dp_1}{dt}\le\frac{-r(x-k)^2}{k\left(1+mz\right)}-d_1y-\left(d_2-\frac{ak\left(1-\alpha z\right)}{b+\left(1-\alpha z\right)x}\right)z$$

Applying constraint 19 gives that, the derivative of $p_1(x,y,z)$ will be negative definite. Therefore, p_1 is a Lypunov function, and the A.EP is a GAS. □

Theorem 3: Suppose that system 1 has a unique P.EP that is LAS, then it has a basin of attraction that satisfies the following constraints:

$$\frac{r}{R_1} < \frac{abz\left(1-\alpha z\right)}{R_2R_2^*}+\frac{r\left(x+x^*\right)}{kR_1} \quad (21)$$

$$q_{12}{}^2 < q_{11}q_{22} \quad (22)$$

$$q_{13}{}^2 < q_{11}q_{33} \quad (23)$$

$$q_{23}{}^2 < q_{22}q_{33} \quad (24)$$

Proof: Consider the following function

$$p_2(x,y,z)=\frac{(x-x^*)^2}{2}+\frac{\left(y-y^*\right)^2}{2}+\frac{(z-z^*)^2}{2} \quad (25)$$

Clearly, the function p_2 is positive definite. So, $p_2(x^*,y^*,z^*)=0$ and $p_2(x,y,z)>0,\ \forall\ (x,y,z)\in R_+^3$ with $(x,y,z)\neq(x^*,y^*,z^*)$. Now, Eq. (25) is derived with respect to t, and by using several simple computations, it's obtained

$$\frac{dp_2}{dt}=(x-x^*)\left(\frac{rx}{1+mz}\left(1-\frac{x}{k}\right)-\frac{a\left(1-\alpha z\right)xz}{b+\left(1-\alpha z\right)x}\right)+\left(y-y^*\right)\left(\frac{ea\left(1-\alpha z\right)xz}{b+\left(1-\alpha z\right)x}-\beta y-d_1y\right)+\left(z-z^*\right)\left(\beta y-d_2z\right),$$

$$\frac{dp_2}{dt}=-q_{11}(x-x^*)^2-q_{22}\left(y-y^*\right)^2-q_{33}\left(z-z^*\right)^2+q_{12}\left(x-x^*\right)\left(y-y^*\right)-q_{13}\left(x-x^*\right)\left(z-z^*\right)-q_{23}\left(y-y^*\right)\left(z-z^*\right)$$

where $q_{11}=\frac{abz(1-\alpha z)}{R_2R_2^*}+\frac{r(x+x^*-k)}{kR_1}$, $q_{22}=\beta+d_1$, $q_{33}=d_2$, $q_{12}=\frac{eabz(1-\alpha z)}{R_2R_2^*}$,

$$q_{13}=\frac{rmx^*\left(k-x^*\right)}{kR_1R_1^*}+\frac{ax^*\left(b+x\right)\left(1-\alpha\left(z+z^*\right)\right)}{R_2R_2^*}+\frac{a\alpha^2xx^*zz^*}{R_2R_2^*},$$

$$q_{23}=\frac{eax^*\left(b+x\right)\left(\alpha\left(z+z^*\right)-1\right)}{R_2R_2^*}-\left(\beta+\frac{ea\alpha^2xx^*zz^*}{R_2R_2^*}\right),$$

with

$$R_1=\left(1+mz\right),\ R_1^*=\left(1+mz^*\right),$$

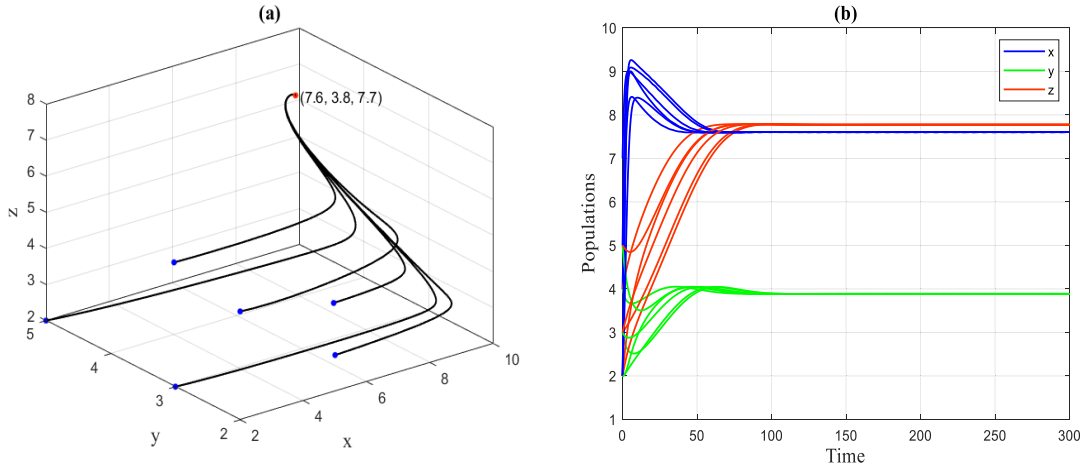

Fig. 2. The system's trajectories 1 with data set 38 and starting from various initial points approach asymptotically $\bar{x}_2 = (7.6, 3.8, 7.7)$. (a) Phase portrait of system 1. (b) Time series of phase portrait (a).

$$R_2 = \left(b + (1 - \alpha z)\, x\right),\ R_2^* = \left(b + \left(1 - \alpha z^*\right) x^*\right).$$

Therefore, under constraints 21–24 gives that

$$\begin{aligned}\frac{dp_2}{dt} \le{}& \frac{-1}{2}\left[\sqrt{q_{11}}\,(x - x^*) - \sqrt{q_{22}}\,(y - y^*)\right]^2 \\ &- \frac{1}{2}\left[\sqrt{q_{11}}\,(x - x^*) + \sqrt{q_{33}}\,(z - z^*)\right]^2 \\ &- \frac{1}{2}\left[\sqrt{q_{22}}\,(y - y^*) + \sqrt{q_{33}}\,(z - z^*)\right]^2\end{aligned}$$

Clearly, the derivative of $p_2(x, y, z)$ will be negative definite and p_2 is a Lypunov function. Furthermore, P.EP is a GAS in the interior of a basin of attraction. □

Persistence of system 1

In this section, the persistence of system 1 is investigated. So, system 1 persists if all species are present for all positive times. In the next theorem, the method given by Freedman and Waltman[35] which depended on the Butler-McGhee lemma is applied to system 1.

Theorem 4: System 1 persists provided that the following constraint holds

$$d_2 < \frac{\beta e a k}{(b + k)\ (\beta + d_1)} \tag{26}$$

Proof: Presume that p is a point belonging to the $Int.\ R_+^3$ and $O(p)$ is the orbit via p.

The omega limit set of the $O(p)$, is denoted by $\Omega(p)$. Then, according to Theorem 1, the $\Omega(p)$ is bounded.

Just now, to show that $\bar{x}_0 \notin \Omega(p)$, suppose the opposite.

Due to $\bar{x}_0$ is a saddle point and by using the Butler-McGhee lemma, there exists at least one other point p_0 belonging to the stable manifold of $\bar{x}_0$ ($\omega^s(\bar{x}_0)$) and $\Omega(p)$.

Moreover, $\omega^s(\bar{x}_0)$ represents the $R_+^2(yz)$ space and $O(p_0)$ is the entire orbit via p_0 contained in $\Omega(p)$.

Now, if p_0 is lying on one of the boundary axes of $R_+^2(yz)$, then the positive particular axis is contained in $\Omega(p)$, which leads to a contradiction with boundedness.

On the other hand, p_0 belongs to the $Int.\ R_+^2(yz)$ and due to the non-existence of an equilibrium point in the $Int.\ R_+^2(yz)$ the orbit via p_0 that is contained in $\Omega(p)$ has to be unbounded which guides to contradiction. Therefore, $\bar{x}_0 \notin \Omega(p)$.

Just now, to show that $\bar{x}_1 \notin \Omega(p)$, suppose the opposite too.

Due to $\bar{x}_1$ is a saddle point if the above constraint 26 holds and by using the Butler-McGhee lemma, then $p_1 \cup \omega^s(\bar{x}_1) \cap \Omega(p)$. Moreover, since $\omega^s(\bar{x}_1)$ is $R_+^2(xy)$ space (similarly, $R_+^2(xz)$ space).

Note that, if p_1 is lying on one of the boundary axes of $R_+^2(xy)$, it is obtained contradiction such as in the above part of the proof. Whilst if $p_1 \in Int.R_+^2(xy)$, then due to the non-existence of an equilibrium point in $Int.\ R_+^2(xy)$ then $O(p_1) \subset \Omega(p)$ is unbounded which contradicts with the bound of $\Omega(p)$. Therefore, $\bar{x}_1 \notin \Omega(p)$.

So $\Omega(p)$ has to be in the $Int.\ R_+^3$, which ensures the persistence of system 1. □

Local bifurcation

A bifurcation occurs when a small variation in parameter values results in a large transformation in

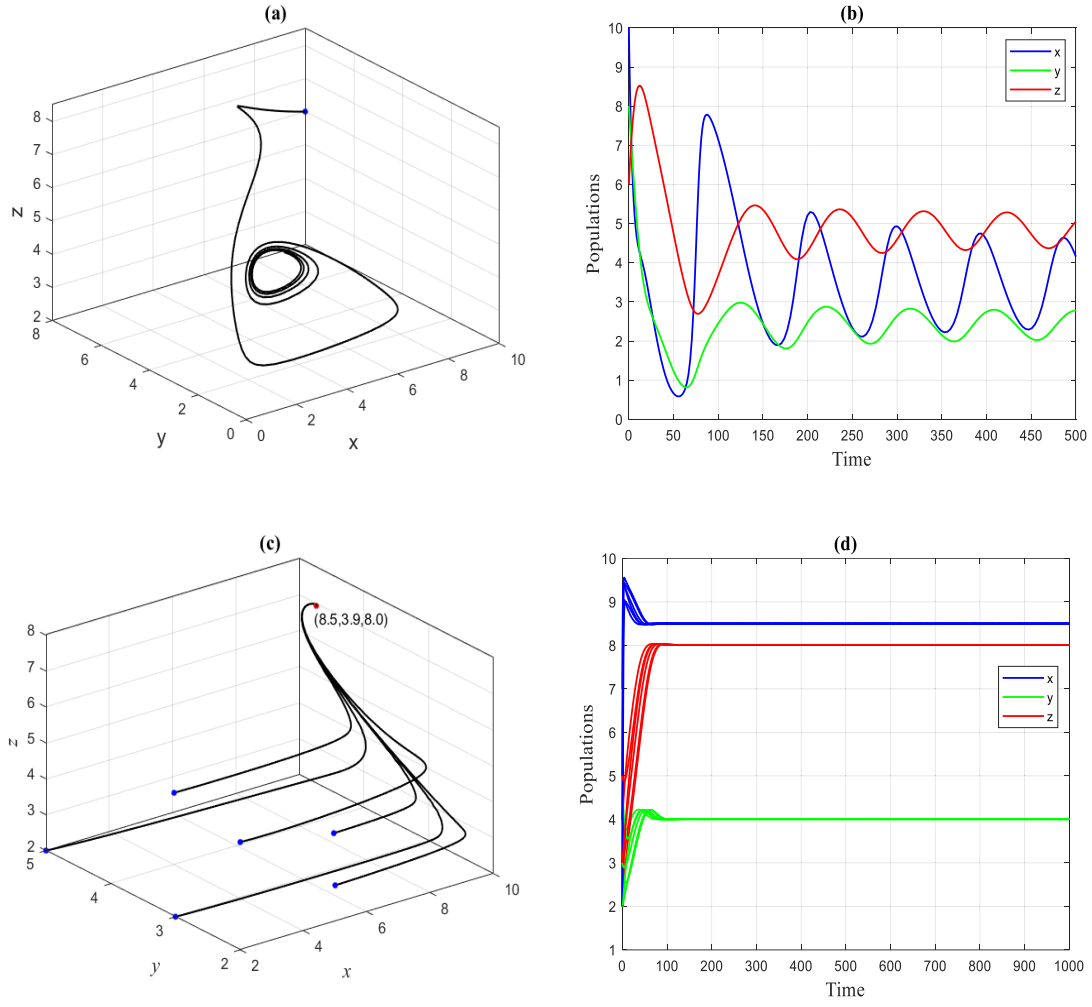

Fig. 3. The system's trajectories 1 with data set 38 and starting from various initial points with different values of r. (a) Phase portrait approaches to periodic attractor for r = 0.8. (b) Time series of phase portrait (a). (c) Phase portrait approaches to P.EP for r = 3. (d) Time series of phase portrait (c).

the system's behavior. In this part, Sotomayor's theorem[36] is used to investigate the local bifurcation near the EP of system 1. There are three types of local bifurcation, such as saddle-node bifurcation (S-NB), transcritical bifurcation (TB), and pitchfork bifurcation (PB). Now, the presence of non-hyperbolic EP is a necessary condition but not sufficient for bifurcation to happen. Therefore, the elect bifurcation parameter is picked so that the EP will be non-hyperbolic at a particular value of that parameter. Now, system 1 can be rewritten in the form

$$\frac{d\boldsymbol{X}}{dt} = \boldsymbol{F}(\boldsymbol{X}) \tag{27}$$

with $\mathbf{X} = (x, y, z)^T$, $\boldsymbol{F} = (F_1, F_2, F_3)^T$. Then depending on the J.M of system 1, simple computation appears that for any non-zero vector $V = (v_1, v_2, v_3)^T$), it is obtained from the next second and third directional derivative

$$D^2F(x, y, z)(V, V) = [\tau_{ij}]_{3\times 1} \tag{28}$$

where

$$\tau_{11} = 2\left[\frac{-r}{k(1+mz)} + \frac{abz(1-\alpha z)^2}{(b+(1-\alpha z)x)^3}\right]v_1{}^2$$
$$+2\left[\frac{-rm(k-2x)}{k(1+mz)^2} + \left(\frac{-ab(b+x)+ab\alpha z(2b+x)}{(b+(1-\alpha z)x)^3}\right)\right]$$
$$\times v_1v_3 + 2\left[\frac{rm^2x}{(1+mz)^3}\left(1-\frac{x}{k}\right) + \frac{ab\alpha x(b+x)}{(b+(1-\alpha z)x)^3}\right]v_3{}^2,$$

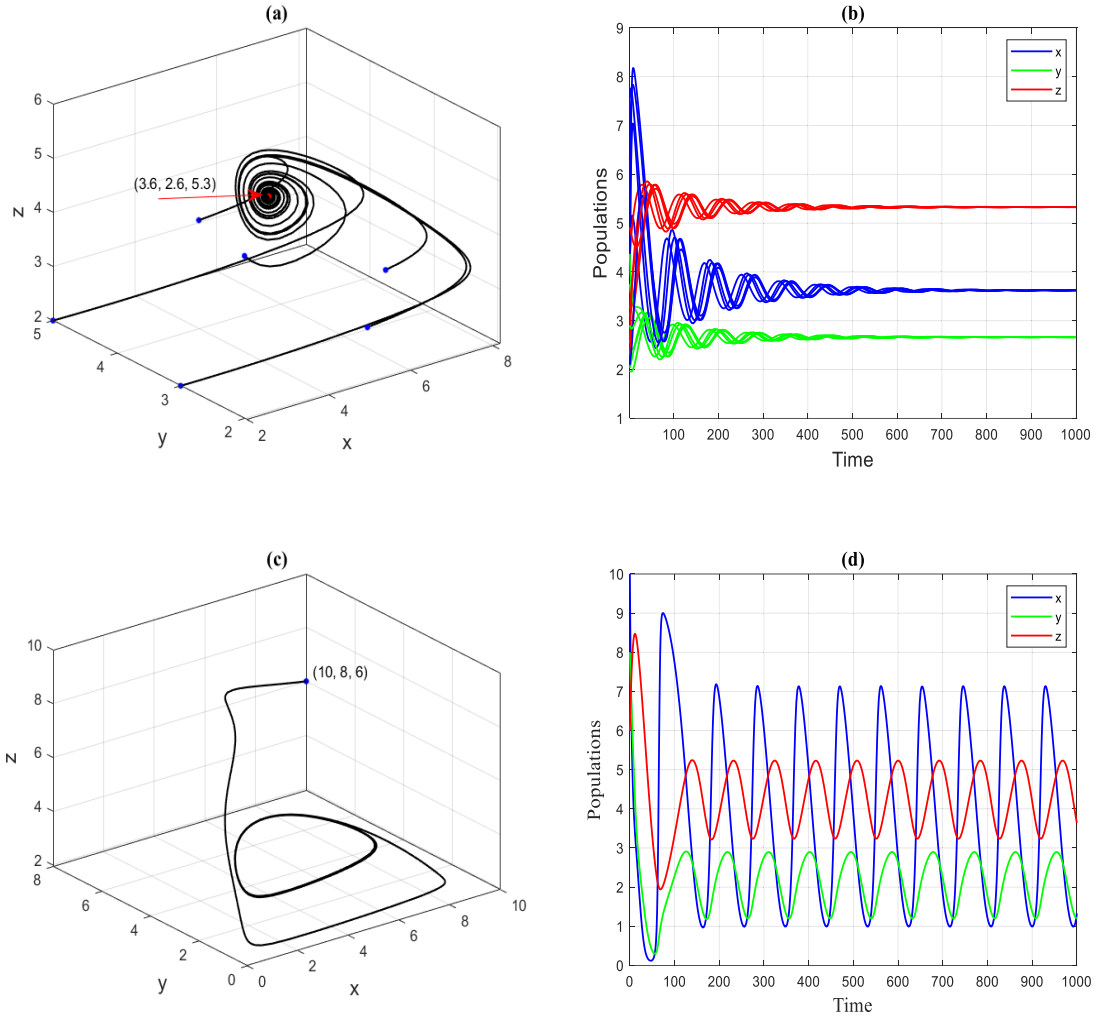

Fig. 4. The system's trajectories 1 with data set 38 and starting from various initial points with different values of m. (a) Phase portrait approaches to P.EP for $m = 0.7$. (b) Time series of phase portrait (a). (c) Phase portrait approaches to periodic attractor for $m = 0.9$. (d) Time series of phase portrait (c).

$$\tau_{21} = 2\left[\frac{-eabz(1-\alpha z)^2}{\left(b+(1-\alpha z)x\right)^3}\right]{v_1}^2 + 2\left[\frac{eab\left(b+x\right)-eab\alpha z\left(2b+x\right)}{\left(b+(1-\alpha z)x\right)^3}\right]v_1v_3 - 2\left[\frac{be a\alpha x\left(b+x\right)}{\left(b+(1-\alpha z)x\right)^3}\right]{v_3}^2,$$

$$\tau_{31} = 0.$$

Theorem 5: System 1 at A.EP possesses a TB when the parameter d_2 passes through the value $d_2^* = \frac{\beta eak}{(b+k)(\beta+d_1)}$.

Proof: From the $J(\bar{x}_1)$ which is given in Eq. (9), system 1 at A.EP and $d_2 = d_2^*$ possess the following J.M denoted by, $J(\bar{x}_1, d_2^*)$

$$J\left(\bar{x}_1, d_2^*\right) = \begin{bmatrix} -r & 0 & \frac{-ak}{b+k} \\ 0 & -(\beta+d_1) & \frac{eak}{b+k} \\ 0 & \beta & -\frac{\beta eak}{(b+k)(\beta+d_1)} \end{bmatrix}$$

Now, A.EP is a non-hyperbolic point since $J(\bar{x}_1, d_2^*)$ has a zero eigenvalue denoted by $\lambda_z^* = 0$ (which means the eigenvalue in the $z-$direction).

let $\boldsymbol{V}^{[1]} = (v_1^{[1]}, v_2^{[1]}, v_3^{[1]})^T$ is the eigenvector corresponding to $\lambda_z^* = 0$.

Consequently $J(\bar{x}_1, d_2^*)\boldsymbol{V}^{[1]} = \boldsymbol{0}$ leads to $\boldsymbol{V}^{[1]} = (\xi_1 v_3^{[1]}, \xi_2 v_3^{[1]}, v_3^{[1]})^T$ where $\xi_1 = -\frac{ak}{r(b+k)} < 0$, $\xi_2 = \frac{eak}{(b+k)(\beta+d_1)} > 0$ and $v_3^{[1]}$ is any non-zero real number.

As well, let $\boldsymbol{\varphi}^{[1]} = (\varphi_1^{[1]}, \varphi_2^{[1]}, \varphi_3^{[1]})^T$ is the eigenvector corresponding to $\lambda_z^* = 0$ of $J(\bar{x}_1, d_2^*)^T$.

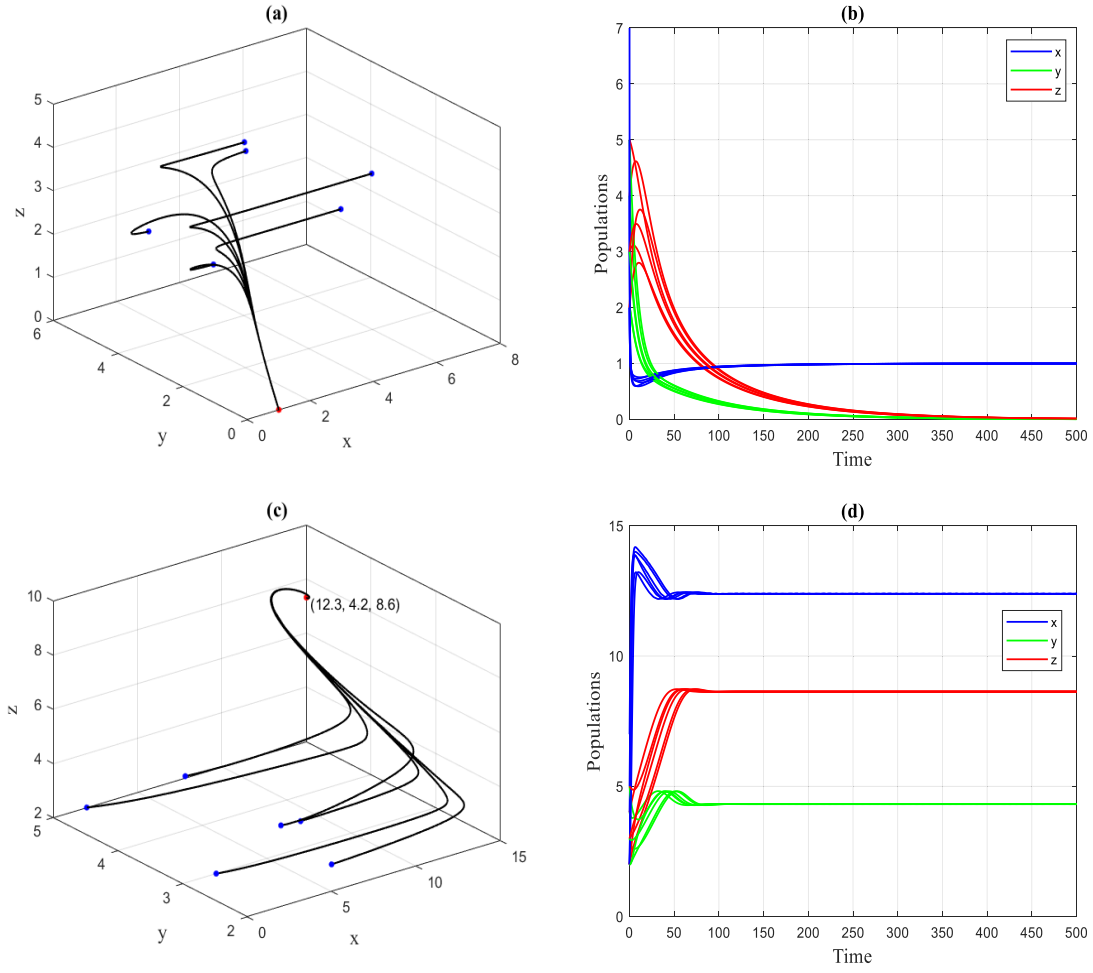

Fig. 5. The system's trajectories 1 with data set 38 and starting from various initial points with different values of k. (a) Phase portrait approaches to A.EP for k = 1. (b) Time series of phase portrait (a). (c) Phase portrait approaches to P. EP for k = 15. (d) Time series of phase portrait (c).

Therefore, $J(\bar{x}_1, d_2^*)^T \boldsymbol{\varphi}^{[1]} = \mathbf{0}$ leads to $\boldsymbol{\varphi}^{[1]} = (0, \delta\varphi_3^{[1]}, \varphi_3^{[1]})^T$ where $\delta = \frac{\beta}{(\beta+d_1)} > 0$ and $\varphi_3^{[1]}$ any non-zero real number.

Moreover,

$$\frac{\partial \boldsymbol{F}}{\partial d_2} = (0, 0, -z)^T$$

Then $\frac{\partial \boldsymbol{F}}{\partial d_2}(\bar{x}_1, d_2^*) = (0, 0, 0)^T$, which leads to $(\boldsymbol{\varphi}^{[1]})^T \frac{\partial \boldsymbol{F}}{\partial d_2}(\bar{x}_1, d_2^*) = 0$. Furthermore,

$$D\frac{\partial \boldsymbol{F}}{\partial d_2}(\bar{x}_1, d_2^*) = \begin{bmatrix} 0 & 0 & 0 \\ 0 & 0 & 0 \\ 0 & 0 & -1 \end{bmatrix}$$

Then,

$$(\boldsymbol{\varphi}^{[1]})^T \left(D\frac{\partial \boldsymbol{F}}{\partial d_2}(\bar{x}_1, d_2^*)\, \boldsymbol{V}^{[1]} \right) = -\varphi_3^{[1]} v_3^{[1]} \neq 0.$$

Over and above that using Eq. (28) with $\bar{x}_1, d_2^*$ and $\boldsymbol{V}^{[1]}$ gives $D^2\boldsymbol{F}(\bar{x}_1, d_2^*)(\boldsymbol{V}^{[1]}, \boldsymbol{V}^{[1]}) = 2(v_3^{[1]})^2(\frac{-r\xi_1^2}{k} + (rm - \frac{ab}{(b+k)^2})\xi_1 + \frac{\alpha abk}{(b+k)^2}, \frac{eab\xi_1}{(b+k)^2} - \frac{eab\alpha k}{(b+k)^2}, 0)^T$

Then

$$(\boldsymbol{\varphi}^{[1]})^T D^2\boldsymbol{F}(\bar{x}_1, d_2^*)(\boldsymbol{V}^{[1]}, \boldsymbol{V}^{[1]}) = \frac{2\,\delta eab}{(b+k)^2}(\xi_1 - \alpha k)\,\varphi_3^{[1]}\left(v_3^{[1]}\right)^2 \neq 0.$$

Therefore, according to Sotomayor's theorem, system 1 at $\bar{x}_1$ has a TB as the parameter d_2 passes via the bifurcation value d_2^*. □

Theorem 6: Presume that constraints 16–17 and the following sufficient constraints are hold then, system 1 at P.EP possesses a S-NB when the parameter r passes through the value $r^* = \frac{k(1+mz^*)}{(k-2x^*)}(Q + \frac{abz^*(1-\alpha z^*)}{(b+(1-\alpha z^*)x^*)^2})$, where $Q = \frac{a_{13}a_{21}a_{32}}{a_{23}a_{32}-a_{22}a_{33}}$,

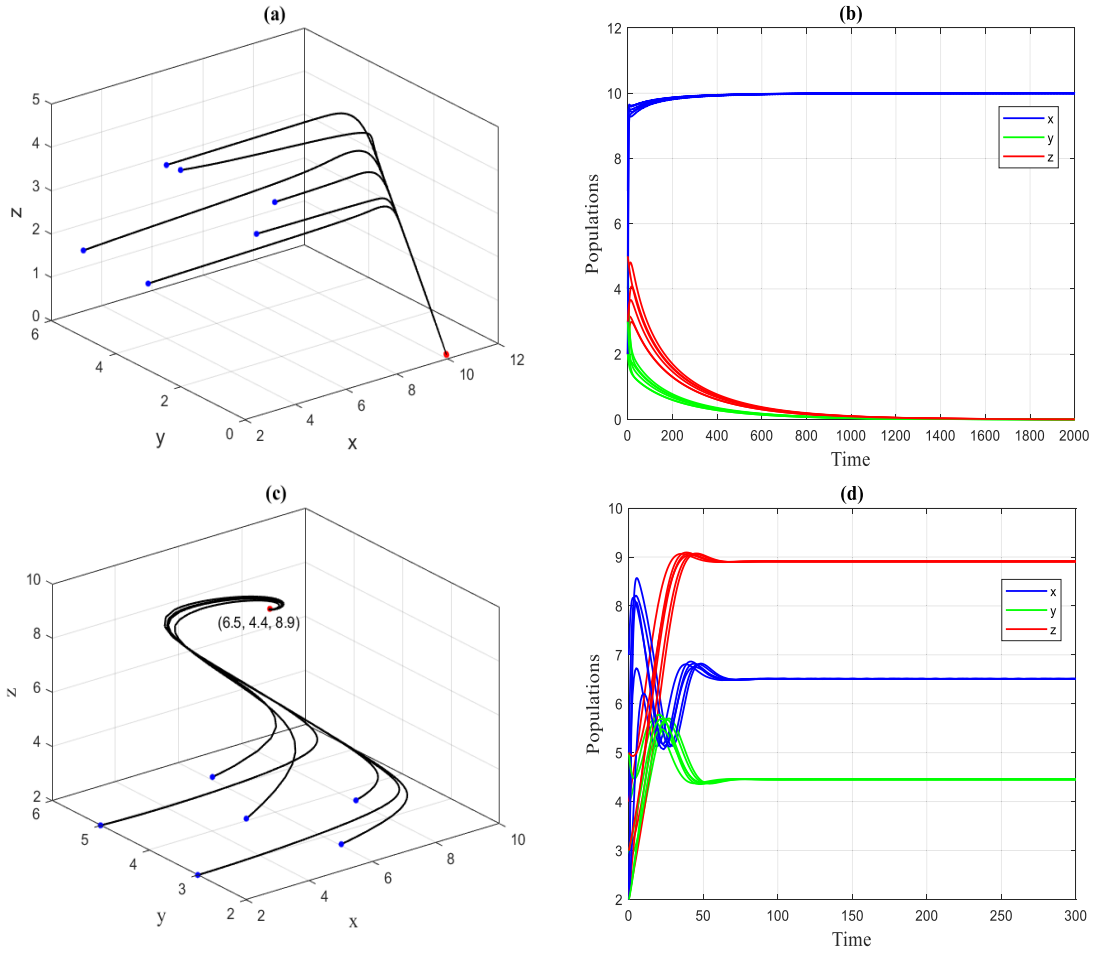

Fig. 6. The system's trajectories 1 with data set 38 and starting from various initial points with different values of a. (a) Phase portrait approaches to A.EP for a = 0.2. (b) Time series of phase portrait (a). (c) Phase portrait approaches to P. EP for a = 0.7. (d) Time series of phase portrait (c).

a_{ij}, $\forall i, j = 1, 2, 3, 4$ are the elements of J.M given by Eq. (12).

$$2x^* < k \tag{29}$$

$$\delta_1 \left(\frac{-r^* \eta_1^2}{k\,(1+mz^*)} + \frac{abz^*(1-\alpha z^*)^2 \eta_1^2}{\left(b+(1-\alpha z^*)\,x^*\right)^3} - \frac{r^* m \eta_1 \left(k-2x^*\right)}{k(1+mz^*)^2} \right.$$
$$+ \frac{-ab\eta_1 \left(b+x^*\right) + ab\eta_1 \alpha z^* \left(2b+x^*\right)}{\left(b+(1-\alpha z^*)\,x^*\right)^3}$$
$$\left. + \frac{r^* m^2 x^*}{(1+mz^*)^3} \left(1 - \frac{x^*}{k}\right) + \frac{ab\alpha x^* \left(b+x^*\right)}{\left(b+(1-\alpha z^*)\,x^*\right)^3} \right)$$
$$+ \delta_2 \left(\frac{-eabz^* \eta_1^2 (1-\alpha z^*)^2}{\left(b+(1-\alpha z^*)\,x^*\right)^3} \right.$$
$$\left. + \frac{eab\left(b+x^*\right)\eta_1 - eab\alpha z^* \eta_1 \left(2b+x^*\right)}{\left(b+(1-\alpha z^*)\,x^*\right)^3} \right.$$
$$\left. - \frac{bea\alpha x^* \left(b+x^*\right)}{\left(b+(1-\alpha z^*)\,x^*\right)^3} \right) \neq 0 \tag{30}$$

Proof. From the $J(\bar{x}_2)$ which is given in Eq. (12), system 1 at P.EP and $r = r^*$ possess the following J.M denoted by, $J(\bar{x}_2, r^*)$. Simple computation appears that $A_3 = 0$ in the characteristic equation defined by Eq. (13) and then $\bar{x}_2$ be a non-hyperbolic EP with $\lambda_x^* = 0$ (zero eigenvalue).

$$J\left(\bar{x}_2, r^*\right) = \begin{bmatrix} Q & 0 & a_{13} \\ a_{21} & a_{22} & a_{23} \\ 0 & a_{32} & a_{33} \end{bmatrix}$$

let $\boldsymbol{V}^{[2]} = (v_1^{[2]}, v_2^{[2]}, v_3^{[2]})^T$ is the eigenvector corresponding to $\lambda_x^* = 0$.

Consequently $J(\bar{x}_2, r^*)\boldsymbol{V}^{[2]} = \boldsymbol{0}$ leads to $\boldsymbol{V}^{[2]} = (\gamma_1 v_3^{[2]}, \gamma_2 v_3^{[2]}, v_3^{[2]})^T$ where $\gamma_1 = -\frac{a_{13}}{Q} > 0$, $\gamma_2 = \frac{a_{13}a_{21} - a_{23}Q}{a_{22}Q} > 0$ and $v_3^{[2]}$ is any non-zero real number.

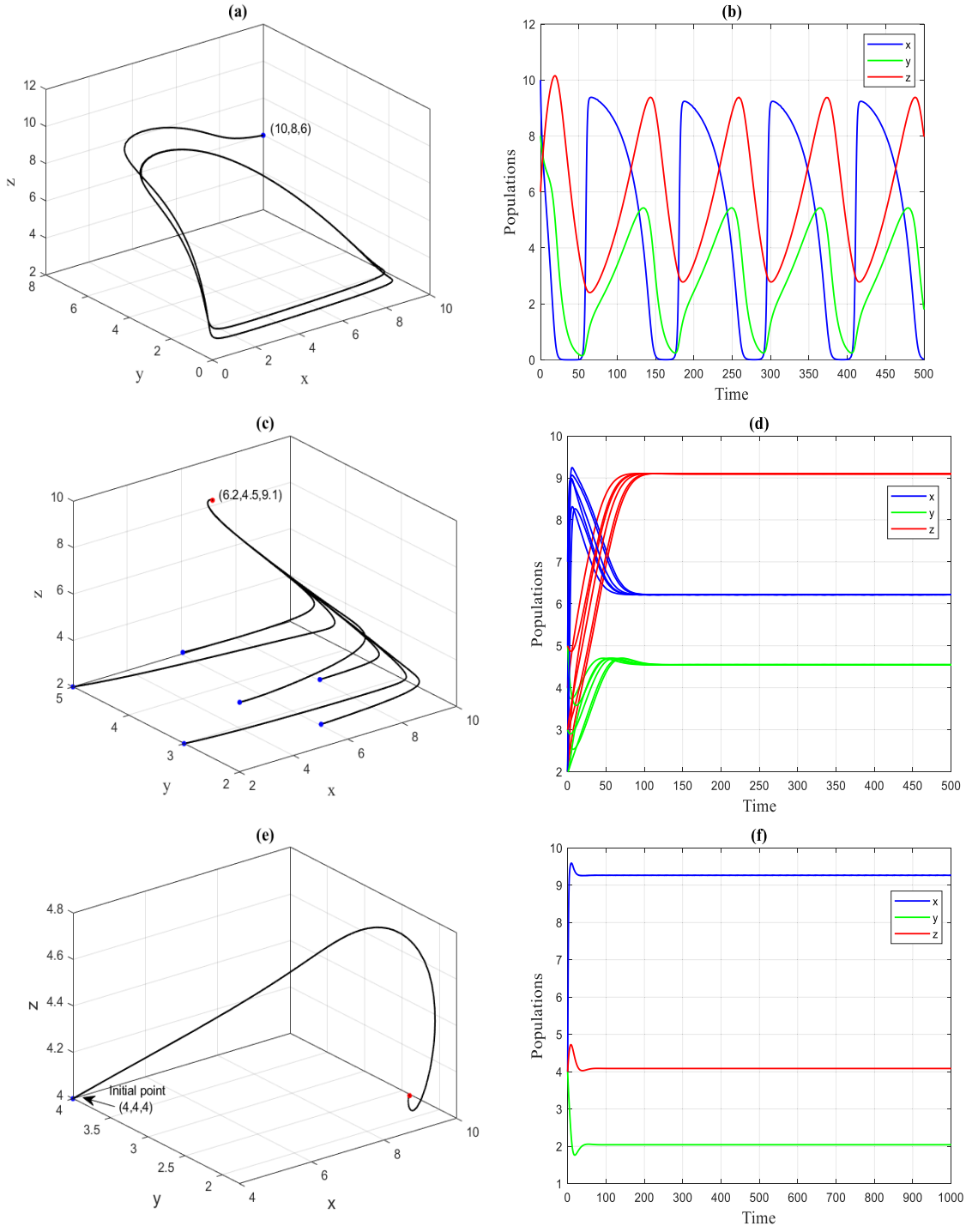

Fig. 7. The system's trajectories 1 with data set 38 and starting from various initial points with different values of b. (a) Phase portrait approaches to P.EP for b = 10. (b) Time series of phase portrait (a). (c) Phase portrait approaches to A. EP for b = 14. (d) Time series of phase portrait (c).

As well, let $\boldsymbol{\varphi}^{[2]} = (\varphi_1^{[2]}, \varphi_2^{[2]}, \varphi_3^{[2]})^T$ is the eigenvector corresponding to $\lambda_x^* = 0$ of $J(\bar{x}_2, r^*)^T$.

Therefore, $J(\bar{x}_2, r^*)^T \boldsymbol{\varphi}^{[2]} = \mathbf{0}$ leads to $\boldsymbol{\varphi}^{[2]} = (\eta_1 \varphi_3^{[2]}, \eta_2 \varphi_3^{[2]}, \varphi_3^{[2]})^T$ where $\eta_1 = \frac{-a_{21}}{Q} < 0$, $\eta_2 = \frac{-a_{32}}{a_{22}} > 0$ and $\varphi_3^{[2]}$ any non-zero real number.

Moreover,

$$\frac{\partial \boldsymbol{F}}{\partial r} = \left(\frac{x}{(1+mz)} \left(1 - \frac{x}{k}\right), 0, 0 \right)^T$$

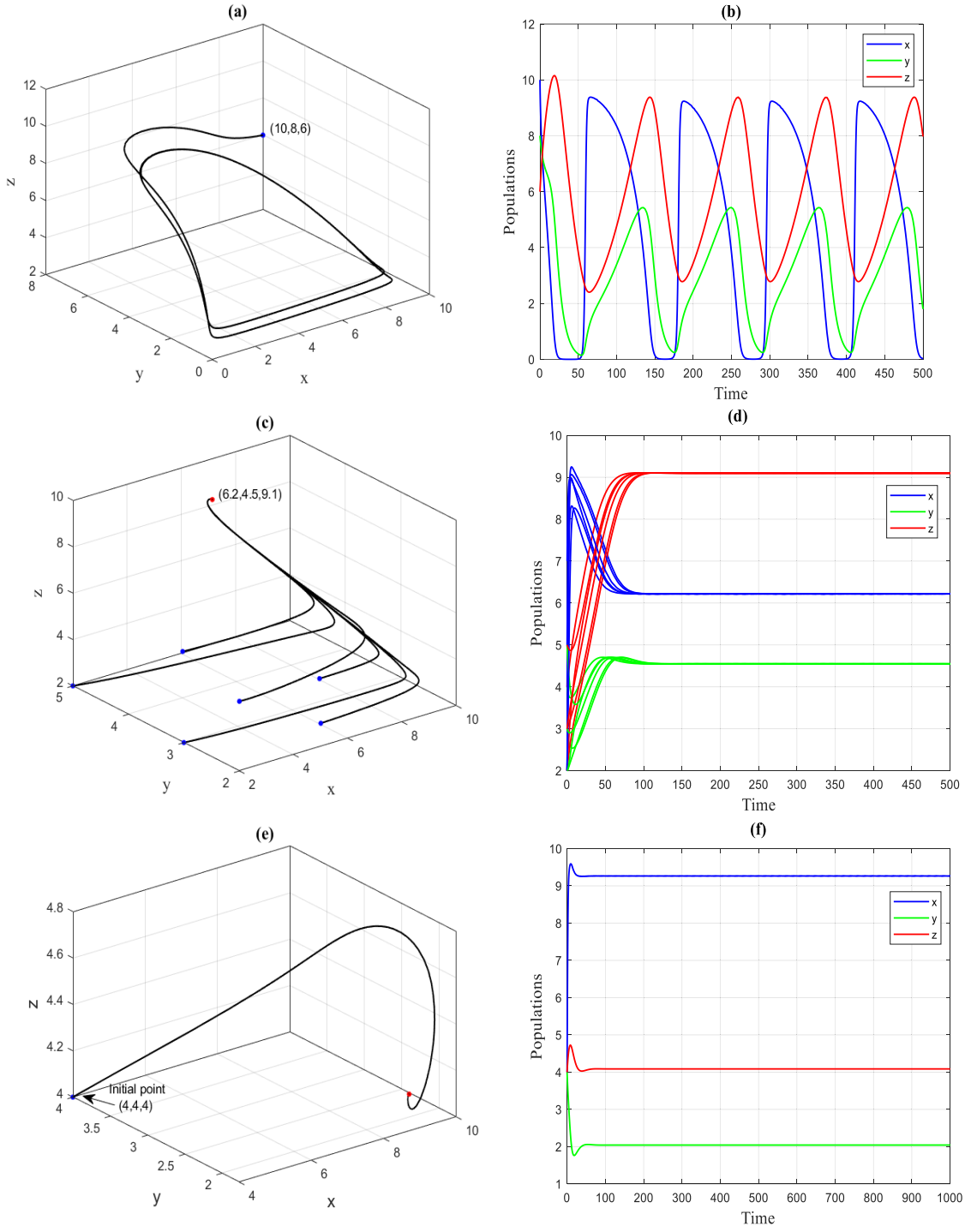

Fig. 8. The system's trajectories 1 with data set 38 and starting from various initial points with different values of α. (a) Phase portrait approaches to periodic attractor for $\alpha = 0.04$. (b) Time series of phase portrait (a). (c) Phase portrait approaches to P. EP for $\alpha = 0.08$. (d) Time series of phase portrait (c). (e) Phase portrait approaches to P. EP for $\alpha = 0.2$ at initial point (4, 4, 4). (f) Time series of phase portrait (e). (g) System 1 approaches asymptotically to chaotic attractor for $\alpha = 0.2$ at initial point (6, 6, 6). (h) Time series of phase portrait (g). (I) System 1 is bi-stable between two forms of attractors P.EP and chaotic attractor for $\alpha = 0.2$.

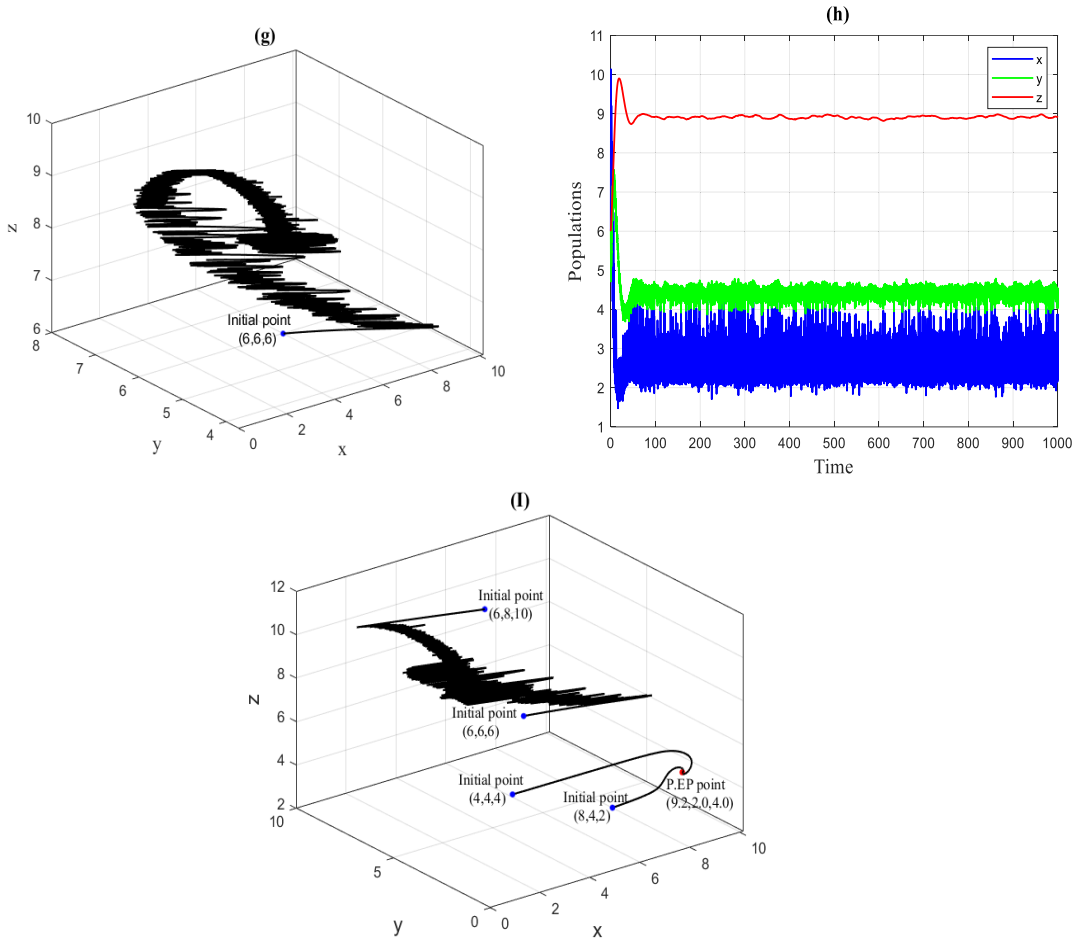

Fig. 8. Continued.

Then $\frac{\partial \boldsymbol{F}}{\partial r}(\bar{x}_2, r^*) = (\frac{x^*}{(1+mz^*)}(1-\frac{x^*}{k}), 0, 0)^T$, which leads to

$$\left(\boldsymbol{\varphi}^{[2]}\right)^T \frac{\partial \boldsymbol{F}}{\partial r}\left(\bar{x}_2, r^*\right) = \frac{x^*}{(1+mz^*)}\left(1-\frac{x^*}{k}\right)\eta_1\varphi_3^{[2]} \neq 0.$$

So, applying Sotomayor's theorem, system 1 has the first constraint of S-NB. While the TB and PB cannot happen at $r = r^*$.

Furthermore, using Eq. (28) with $\bar{x}_2, r^*$ and $\boldsymbol{V}^{[2]}$ gives

$$\left(\boldsymbol{\varphi}^{[2]}\right)^T D^2\boldsymbol{F}\left(\bar{x}_2, r^*\right)\left(\boldsymbol{V}^{[2]}, \boldsymbol{V}^{[2]}\right) = 2\varphi_3^{[2]}\left(v_3^{[2]}\right)^2$$
$$\times\left[\delta_1\left(\frac{-r^*\eta_1^2}{k\left(1+mz^*\right)} + \frac{abz^*(1-\alpha z^*)^2\eta_1^2}{\left(b+(1-\alpha z^*)x^*\right)^3}\right.\right.$$
$$-\frac{r^*m\eta_1\left(k-2x^*\right)}{k(1+mz^*)^2} + \frac{-ab\eta_1\left(b+x^*\right)+ab\eta_1\alpha z^*\left(2b+x^*\right)}{\left(b+(1-\alpha z^*)x^*\right)^3}$$
$$\left.+\frac{r^*m^2x^*}{(1+mz^*)^3}\left(1-\frac{x^*}{k}\right) + \frac{ab\alpha x^*\left(b+x^*\right)}{\left(b+(1-\alpha z^*)x^*\right)^3}\right)$$
$$+\delta_2\left(\frac{-eabz^*\eta_1^2(1-\alpha z^*)^2}{\left(b+(1-\alpha z^*)x^*\right)^3}\right.$$
$$+\frac{eab\left(b+x^*\right)\eta_1 - eab\alpha z^*\eta_1\left(2b+x^*\right)}{\left(b+(1-\alpha z^*)x^*\right)^3}$$
$$\left.\left.-\frac{bea\alpha x^*\left(b+x^*\right)}{\left(b+(1-\alpha z^*)x^*\right)^3}\right)\right]$$

Obviously, due to constraint 30 leads to $(\boldsymbol{\varphi}^{[2]})^T D^2\boldsymbol{F}(\bar{x}_2, r^*)(\boldsymbol{V}^{[2]}, \boldsymbol{V}^{[2]}) \neq 0$. Therefore, according to Sotomayor's theorem, system 1 at $\bar{x}_2$ has a S-NB as the parameter r passes via the bifurcation value r^*. Otherwise, if constraint 30 is not valid, then system 1 has no any type of bifurcation. □

Theorem 7: Presume that constraints 15–17 along with the following sufficient constraints hold

$$W_1 + W_2 < 0 \tag{31}$$

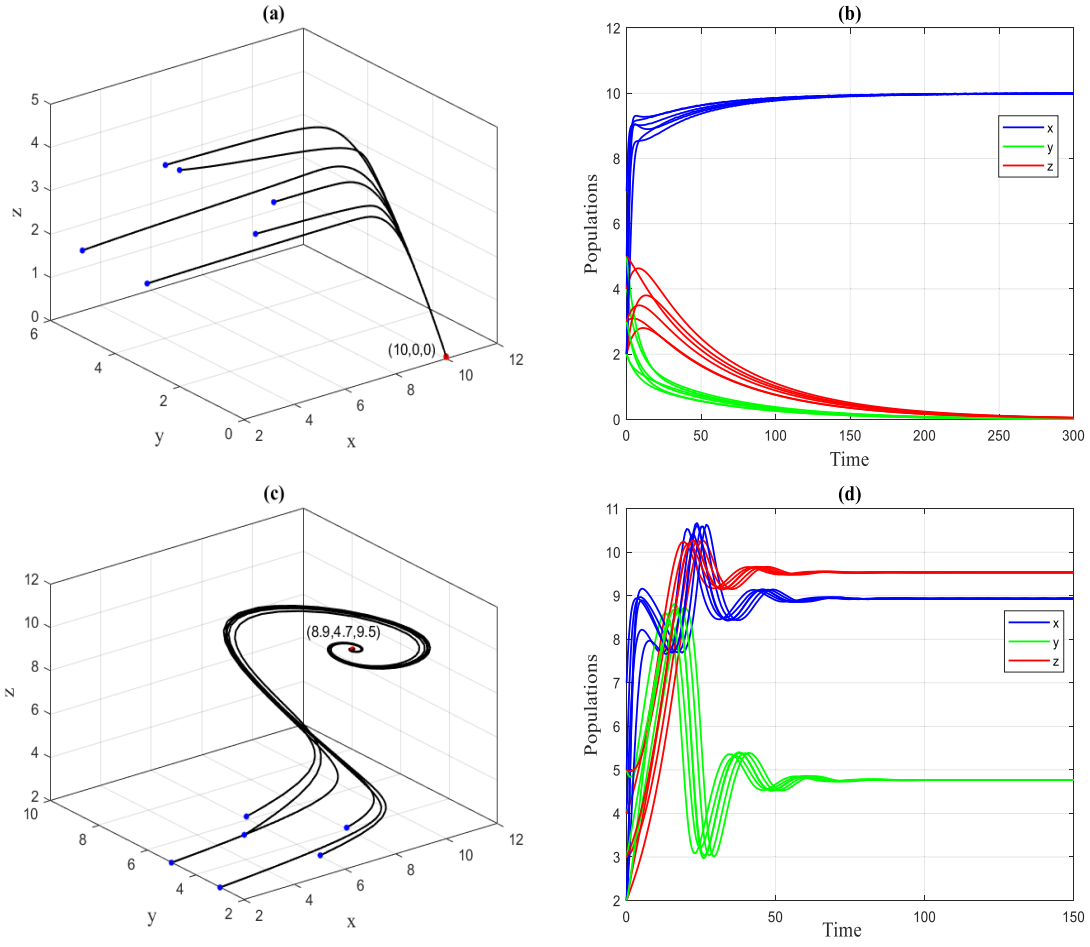

Fig. 9. The system's trajectories 1 with data set 38 and starting from various initial points with different values of e. (a) Phase portrait approaches to A.EP for e = 0.1. (b) Time series of phase portrait (a). (c) Phase portrait approaches to P. EP for e = 0.8. (d) Time series of phase portrait (c).

$$p_3 < 0 \tag{32}$$

$$\left[H_1\left(d_2^*\right)H_2\left(d_2^*\right)\right]' < H_3{}'\left(d_2^*\right) \tag{33}$$

where $H_i; i = 1, 2, 3$ are illustrated in Eq. (13) and $W_1 + W_2$ given in Eq. (14). System 1 undergoes a Hopf bifurcation (H.B) around the equilibrium point $\bar{x}_2$ as the parameter d_2 passes through the positive value d_2^*.

Proof: According to the H.B theorem[36] for the three autonomous systems, system 1 undergoes a H.B as the parameter d_2 passes via the positive value d_2^* provided that:

The $J(\bar{x}_2)$ of system 1 has a pair of complex eigenvalues which are simple $\rho_1(d_2) \pm i\rho_2(d_2)$, they convert purely imaginary at $d_2 = d_2^*$, while the 3rd eigenvalue rests real and negative. Furthermore, the transversality constraint $\frac{d\rho_1(d_2)}{dd_2}|_{\,d_2=d_2^*} \neq 0$ should be met.

The above 1st constraint will be satisfied if the following constraint met $\Delta = H_1H_2 - H_3 = 0$, which represented the coefficients of the characteristic equation illustrated by Eq. (13). Using simple computations, it would be obtained as equivalent to

$$p_1{d_2}^2 + p_2d_2 + p_3 = 0 \tag{34}$$

where $p_1 = -(a_{11} + a_{22}) > 0$,

$p_2 = (a_{11} + a_{22})^2 - a_{23}a_{32}$,

$p_3 = -a_{11}a_{22}\,(a_{11} + a_{22}) + a_{32}\,(a_{22}a_{23} + a_{13}a_{21})$.

Obviously, by using the signs of elements of $J(\bar{x}_2)$ that given in Eq. (12) with the sufficient constraints 15–16, 31, and 32 which leads to $a_{11} < 0$, $a_{13} < 0$, $a_{23} > 0$, $W_1 + W_2 < 0$, and $p_3 < 0$, therefore Eq. (34) has a unique positive root represented by d_2^* that satisfies $H_1(d_2^*)H_2(d_2^*) = H_3(d_2^*)$. Moreover, as

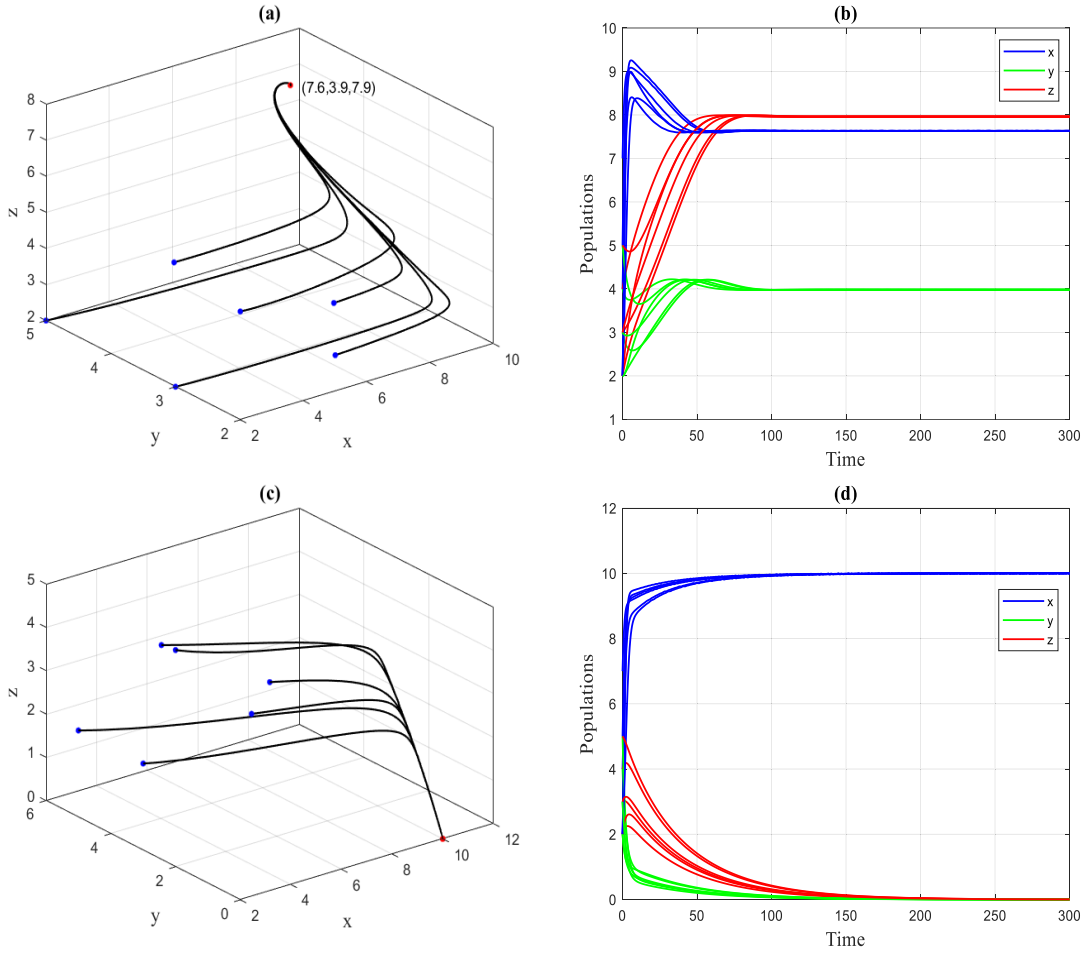

Fig. 10. The system's trajectories 1 with data set 38 and starting from various initial points with different values of d_1. (a) Phase portrait approaches to P. EP for $d_1 = 0.005$. (b) Time series of phase portrait (a). (c) Phase portrait approaches to A.EP for $d_1 = 0.3$ (d) Time series of phase portrait (c).

$d_2 = d_2^*$ then the characteristic Eq. (13) will be

$$(\lambda + H_1)\left(\lambda^2 + H_2\right) = 0 \tag{35}$$

So, Eq. (35) has the next roots

$$\lambda_1 = -H_1\left(d_2^*\right) \text{ and } \lambda_{2,3} = \pm i\sqrt{H_2\left(d_2^*\right)} = \pm i\rho_2\left(d_2^*\right).$$

Again, by using the signs of elements of $J(\bar{x}_2)$ with the given constraint 17 guarantees that $H_i > 0$ for all $i = 1, 2, 3$. Therefore, the 1st constraint of the H.B follows.

Presently to investigate the occurrence of the transversality constraint, replace $\rho_1(d_2) + i\rho_2(d_2)$, here d_2 in the neighborhood of d_2^*, in the Eq. (35) with take the derivative concerning d_2 and by comparing the two sides and equaling their real and imaginary parts, it is obtained the following result

$$\begin{aligned} \Psi\left(d_2\right)\rho_1{}'\left(d_2\right) - \Phi\left(d_2\right)\rho_2{}'\left(d_2\right) &= -\Theta\left(d_2\right) \\ \Phi\left(d_2\right)\rho_1{}'\left(d_2\right) + \Psi\left(d_2\right)\rho_2{}'\left(d_2\right) &= -\Gamma\left(d_2\right) \end{aligned} \tag{36}$$

where $\Theta(d_2) = H_1{}'(d_2)[\rho_1(d_2)]^2 - H'(d_2)[\rho_2(d_2)]^2 + H_2{}'(d_2)\rho_1(d_2) + H_3{}'(d)$,

$$\Psi\left(d_2\right) = 3\left[\rho_1\left(d_2\right)\right]^2 + 2H_1\left(d_2\right)\rho_1\left(d_2\right) - 3\left[\rho_2\left(d_2\right)\right]^2 + H_2\left(d_2\right),$$

$$\Gamma\left(d_2\right) = 2H_1{}'\left(d_2\right)\rho_1\left(d_2\right)\rho_2\left(d_2\right) + H_2{}'\left(d_2\right)\rho_2\left(d_2\right),$$

$$\Phi\left(d_2\right) = 6\rho_1\left(d_2\right)\rho_2\left(d_2\right) + 2H_1\left(d_2\right)\rho_2\left(d_2\right).$$

Now, using Cramer's rule for solving the linear system 36 for the unknowns $\rho_1{}'(d_2)$ and $\rho_2{}'(d_2)$ gives

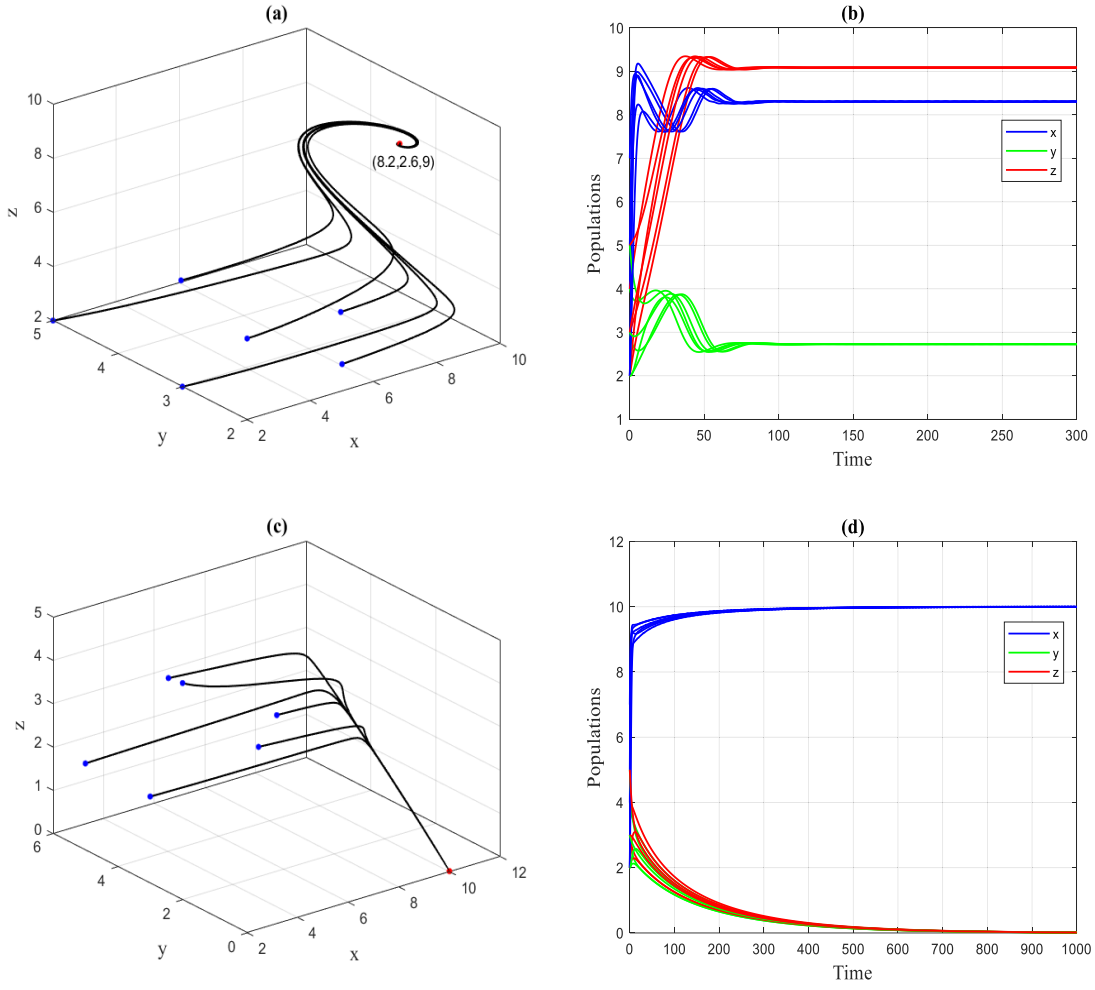

Fig. 11. The system's trajectories 1 with data set 38 and starting from various initial points with different values of d_2. (a) Phase portrait approaches to P. EP for $d_2 = 0.03$. (b) Time series of phase portrait (a). (c) Phase portrait approaches to A.EP for $d_2 = 0.1$ (d) Time series of phase portrait (c).

that

$$\rho_1{}'\left(d_2\right) = -\frac{\Theta\left(d_2\right)\Psi\left(d_2\right) + \Gamma\left(d_2\right)\Phi\left(d_2\right)}{\left[\Psi\left(d_2\right)\right]^2 + \left[\Phi\left(d_2\right)\right]^2},$$

$$\rho_2{}'\left(d_2\right) = -\frac{\Gamma\left(d_2\right)\Psi\left(d_2\right) - \Theta\left(d_2\right)\Phi\left(d_2\right)}{\left[\Psi\left(d_2\right)\right]^2 + \left[\Phi\left(d_2\right)\right]^2} \tag{37}$$

Therefore, the transversality constraint is satisfied if

$$\Theta\left(d_2^*\right)\Psi\left(d_2^*\right) + \Gamma\left(d_2^*\right)\Phi\left(d_2^*\right) \neq 0$$

Clearly, $\rho_1(d_2^*) = 0$ and $\rho_2(d_2^*) = \sqrt{H_2(d_2^*)}$, so that

$$\Theta\left(d_2^*\right) = -H_1{}'\left(d_2^*\right)H_2\left(d_2^*\right) + H_3{}'\left(d_2^*\right),$$

$$\Psi\left(d_2^*\right) = -2H_2\left(d_2^*\right),$$

$$\Gamma\left(d_2^*\right) = H_2{}'\left(d_2^*\right)\sqrt{H_2\left(d_2^*\right)},$$

$$\Phi\left(d_2^*\right) = 2H_1\left(d_2^*\right)\sqrt{H_2\left(d_2^*\right)}.$$

Accordingly, the following result is obtained

$$\rho_1{}'\left(d_2^*\right) = 2H_2\left(d_2^*\right) \times \frac{\left[H_3{}'\left(d_2^*\right) - \left(H_1{}'\left(d_2^*\right)H_2\left(d_2^*\right) + H_1\left(d_2^*\right)H_2{}'\left(d_2^*\right)\right)\right]}{\left[\Psi\left(d_2^*\right)\right]^2 + \left[\Phi\left(d_2^*\right)\right]^2}$$

So, $\rho_1{}'(d_2^*) > 0$ under constraint 33 and then the transversality constraint was met. Therefore H.B occurs at $d_2 = d_2^*$. □

Numerical simulations

Numerical simulation outcomes are equally substantial to those obtained from the analysis. The goal is to confirm the findings analytically and study the impacts of different parameter values on the dynamics behavior of system 1. Each of the numerical simulation outcomes of system 1 appears in some figures using the MATLAB program. Now, the following presumptive set of parameters is utilized.

$$r = 2,\ m = 0.2,\ k = 10,\ a = 0.4,\ \alpha = 0.1, b = 2,$$
$$e = 0.3,\ \beta = 0.1,\ d_1 = 0.01, d_2 = 0.05. \quad (38)$$

It is clear that for the given set of data in Eq. (38) and starting from various initial points, system 1 approaches asymptotically to P. EP, $\bar{x}_2 = (7.6, 3.8, 7.7)$ as illustrated in Fig. 2.

Now, the effect of changing the value of intrinsic growth rate r of system 1 is investigated. Clearly, for $r \in (0, 0.9)$ then the system's trajectory 1 results in a periodic attractor $Int.R_+^3$, which means losing the stability of the P.EP. While for $r \geq 0.9$ then the system's trajectory 1 approaches to P.EP, $\bar{x}_2 = (8.5,\ 3.9,\ 8.0)$. Now, the obtained outcomes are offered at determined values in Fig. 3.

The impact of varying the value of fear rate m of system 1 is studied. It is clear that for $m \in (0, 0.8)$ then the system's trajectory 1 starting from various initial points approaches to P. EP, $\bar{x}_2 = (3.6, 2.6, 5.3)$. However, for $m \geq 0.8$ then the system's trajectory 1 approaches to a periodic attractor in the $Int.\ R_+^3$. Just now, the obtained outcomes are presented at particular values in Fig. 4.

The effect of varying the value of carrying capacity k of system 1 is investigated. Obviously, for $k \in (0, 2)$ then the system's trajectory 1 approaches to A.EP, $\bar{x}_1 = (1, 0, 0)$, which means losing the stability of the P.EP and the extinction of the predators (mature and immature). Furthermore, for $k \geq 2$ then the system's trajectory 1 approaches to P.EP, $\bar{x}_2 = (12.5, 4.2, 8.5)$ in the $Int.\ R_+^3$. The obtained outcomes are presented at particular values in Fig. 5.

The influence of varying the value of the maximum attack rate a of system 1 is studied. Clearly, for $a \in (0, 0.3)$ then the system's trajectory 1 approaches to A.EP, $\bar{x}_1 = (10, 0, 0)$. Moreover, for $a \geq 0.3$ then the system's trajectory 1 approaches to P.EP $\bar{x}_2 = (6.5, 4.4, 8.9)$ in the $Int.\ R_+^3$. The obtained outcomes are presented at particular values in Fig. 6.

The impact of varying the value of half-saturation level b of system 1 is studied. It is clear that for $b \in (1, 10)$ then the system's trajectory 1 approaches to P.EP, $\bar{x}_2 = (9.8, 0.7, 1.4)$. Also, for $b \geq 14$ then the system's trajectory 1 approaches to A.EP $\bar{x}_1 = (10, 0, 0)$. The obtained outcomes are presented at particular values in Fig. 7.

The effect of varying the value of the refuge rate of prey α of system 1 is investigated. For $\alpha \in (0, 0.06)$ then the system's trajectory 1 approaches to a periodic attractor in the $Int.\ R_+^3$. Also, for $\alpha \in [0.06, 0.2)$ then the system's trajectory 1 approaches to P.EP, $\bar{x}_2 = (6.2, 4.5, 9.1)$. Moreover, at the initial points (4, 4, 4) and (6, 6, 6) with $\alpha = 0.2$ leads to the system's trajectory 1 approaches to different attractors P.EP, complex dynamics containing chaos, which means appearing of bi-stable case. The obtained outcomes are presented at particular values in Fig. 8.

The impact of changing the value of the conversion rate e of system 1 is studied. For $e \in (0, 0.2)$ then the system's trajectory 1 approaches to A. EP, $\bar{x}_1 = (10, 0, 0)$. Also, for $e \geq 0.2$ then the system's trajectory 1 approaches to P.EP $\bar{x}_2 = (8.9, 4.7, 9.5)$. The obtained outcomes are presented at particular values in Fig. 9.

The impact of varying the value of the grown-up rate from an immature predator β of system 1 is a quantitative effect, then the system's trajectory 1 approaches asymptotically to the P.EP.

The impact of changing the value of the death rate of immature predator d_1 of system 1 is studied. For $d_1 \in (0, 0.2)$ then the system's trajectory 1 approaches to P.EP, $\bar{x}_2 = (7.6, 3.9, 7.9)$. Also, for $d_1 \geq 0.2$ then the system's trajectory 1 approaches to A.EP $\bar{x}_1 = (10, 0, 0)$. The obtained outcomes are presented at particular values in Fig. 10.

The impact of changing the value of the death rate of mature predator d_2 of system 1 is studied. For $d_2 \in (0, 0.1)$ then the system's trajectory 1 approaches to P.EP, $\bar{x}_2 = (8.2, 2.6, 9.0)$. Also, for $d_2 \geq 0.1$ then the system's trajectory 1 approaches to A.EP $\bar{x}_1 = (10, 0, 0)$. The obtained outcomes are presented at particular values in Fig. 11.

Results and discussion

In this paper, the effect of fear and predator dependent refuge of a prey-predator system with the stage structure of a predator is investigated. The system's behavior is studied theoretically as well as numerically. System 1 contains three non-negative EP denoted by T.EP, A.EP, and P.EP, two of them lying on the boundary axis and the third in the positive quadrant.

The system's behavior of the solution is studied theoretically. The T.EP is detected to be the unstable point (saddle), while the A.EP and P.EP are LAS if constraints 11 and 15–18 are met, respectively.

The persistence constraints are established. The local bifurcation is investigated by using Sotomayor's theorem.

Numerical simulations are used to ensure the theoretical results obtained. By using the hypothetical data given in Eq. (38) the following outcomes are obtained. Beginning from different sets of initial points, the system's trajectories 1 with data in Eq. (38) approach asymptotically to P.EP, this means the theoretical conclusions on the stability of equilibrium are confirmed. Decreasing the intrinsic growth rate r below a critical value leads to losing the stability of the P.EP while system 1 persists at periodic attractor in $Int.\ \mathbb{R}^3_+$. Increasing the fear rate m above a critical value leads to losing the stability of the P.EP, while system 1 persists at periodic attractor in $Int.\ \mathbb{R}^3_+$. Decreasing the carrying capacity k, maximum attack rate a, and conversion rate e below a specific value leads to losing the persistence of system 1 and the trajectory approaches asymptotically to the A.EP. Increasing the half saturation level b, the death rate of immature predator d_1 and death rate of mature predator d_2 above a specific value leads to losing the persistence of system 1 and the trajectory approaches asymptotically to the A.EP. It is observed that decreasing the refuge rate of prey α below the specific value leads to losing the stability of system 1 and it persists at periodic attractor in $Int.\ \mathbb{R}^3_+$, while increasing α above the specific value leads to an approach to different attractors as the solution starts from different initial points (bi-stable case). Decreasing (increasing) the grown-up rate β below (above) a specific value leads to the persisting of system 1 at a P.EP. β has quantitative effects on the dynamic of system 1.

Conclusion

The P.EP is eliminated when the growth rate of prey and refuge decreases below a specific level, which leads to the system approach to periodic attractor in $Int.\ \mathbb{R}^3_+$. While the high level of fear has a destabilizing effect which leads to a periodic attractor in $Int.\ \mathbb{R}^3_+$. On the other side, the rising level of predator-dependent refuge and using different initial points leads to an approach to different attractors (P.EP and complex dynamics containing chaos) which means a bi-stable case. The P.EP is eliminated when the carrying capacity, maximum attack rate, and conversion rate fall below a specific level, which leads to extinction in predators (mature and immature). As a result, trajectories approach asymptotically to the A.EP. When the half saturation level and death rates of immature and mature predators rise above a particular level, then the P.EP is eliminated and trajectories approach asymptotically to the A.EP.

System 1 persists if all species are present for all positive time, which means that the trajectories approach asymptotically to P.EP.

Therefore, the above conclusions illustrated that system 1 is very sensitive to changing the parameters values and initial points (especially). Now, the future direction of this paper will be discussed in the following.

For the proposed model, which consists of a prey-predator model involving the fear effect, predator dependent refuge, and the stage structure in a predator, it is possible to modify it so that it represents different real-world systems that are important to study too. Different types of functional responses can be used for describing the predation process in addition to combining with epidemic diseases that can be contracted by any of their species. Additionally, studying the effect of time delays that affect an ecological system.

Acknowledgment

The authors would like to thank the editor and referees for their worthy comments and propositions, which improved the goodness of this manuscript.

Authors' declaration

- Conflicts of Interest: None.
- We hereby confirm that all the Figures and Tables in the manuscript are ours. Furthermore, any Figures and images, that are not ours, have been included with the necessary permission for republication, which is attached to the manuscript.
- No animal studies are present in the manuscript.
- No human studies are present in the manuscript.
- Ethical Clearance: The project was approved by the local ethical committee at the University of Baghdad.

Authors' contribution statement

G.J. A. and H.A. I. contributed to the idea of the suggested model. G.J. A. performed the calculations. G.J. A. and H.A. I. investigated the analytical methods. Also, both authors contributed to the analysis of the results and the final state of the manuscript.

References

1. Lotka AJ. Elements of Physical Biology. Nature. 1925;116:461. https://doi.org/10.1038/116461b0.

2. Volterra V. Fluctuations in the Abundance of a Species Considered Mathematically. Nature. 1926;118:558–560. https://doi.org/10.1038/118558a0.
3. Naji RK. On The Dynamical Behavior of a Prey-Predator Model with The Effect of Periodic Forcing. Baghdad Sci J. 2021;4(1):147–157.
4. Maghool FH, Naji RK. The Dynamics of a Tritrophic Leslie-Gower Food-Web System with the Effect of Fear. J Appl Math. 2021;2021(1):1–21. https://doi.org/10.1155/2021/2112814.
5. Abdul Satar H, Naji RK. Stability and Bifurcation of a Prey-Predator-Scavenger Model in the Existence of Toxicant and Harvesting. Int J Math Math Sci. 2019;2019:1–17. https://doi.org/10.1155/2019/1573516.
6. Roy P, Upadhyay RK, Caur J. Modeling Zika Transmission Dynamics: Prevention and Control. J Biol Syst. 2020;28(3):719–749. https://doi.org/10.1142/S021833902050014X.
7. Abdul Satar H, Naji RK. A Mathematical Study for the Transmission of Coronavirus Disease. Mathematics. 2023;11(10):2330. https://doi.org/10.3390/math11102330.
8. Kwasi-Do NOO, Afriyie C. The Role of Control Measures and the Environment in the Transmission Dynamics of Cholera. Abst Appl Anal. 2020;2020(1):1–16. https://doi.org/10.1155/2020/2485979.
9. Jamil AM, Naji RK. Modeling and Analyzing the Influence of Fear on the Harvested Modified Leslie-Gower Model. Baghdad Sci J. 2023;20(5):1701–1712. https://doi.org/10.21123/bsj.2023.7432.
10. Guo H, Han J, Zhang G. Hopf Bifurcation and Control for the Bioeconomic Predator-Prey Model with Square Root Functional Response and Nonlinear Prey Harvesting. Mathematics. 2023;11(24):4958. https://doi.org/10.3390/math11244958.
11. Hussien RM, Naji RK. The Dynamics of a Delayed Ecological Model with Predator Refuge and Cannibalism. Commun Math Biol Neurosci. 2023;2023:1–30. https://doi.org/10.28919/cmbn/7988.
12. Ibrahim HA, Naji RK. The Complex Dynamic in Three Species Food Webmodel Involving Stage Structure and Cannibalism. Proceedings of the 2020 2nd International Conference on Sustainable Manufacturing, Materials and Technologies, 17–18 July 2020, Coimbatore, India. AIP Conf Proc. 2020;2292(1):020006. https://doi.org/10.1063/5.0030510.
13. Abdulghafour AS, Naji RK. Modeling and Analysis of a Prey-Predator System Incorporating Fear, Predator-Dependent Refuge, and Cannibalism. Commun Math Biol Neurosci. 2022;2022:1–36. https://doi.org/10.28919/cmbn/7722.
14. Umrao AK, Srivastava PK. Bifurcation Analysis of a Predator–Prey Model with Allee Effect and Fear Effect in Prey and HuntingCooperation in Predator. Differ Equ Dyn Syst. 2023. https://doi.org/10.1007/s12591-023-00663-w.
15. Al-Momen S, Naji RK. The Dynamics of Sokol-Howell Prey-Predator Model Involving Strong Allee Effect. Iraqi J Sci. 2021;62(9):3114–3127. https://doi.org/10.24996/ijs.2021.62.9.27.
16. Arora C, Kumar V. Dynamics of Predator–Prey System with Migrating Species and Disease in Prey Population. Differ Equ Dyn Syst. 2021;29:87–112. https://doi.org/10.1007/s12591-020-00529-5.
17. Sugie J, Saito Y. Uniqueness of Limit Cycles in a Rosenzweig-Macarthur Model with Prey Immigration. SIAM J Appl Math. 2012;72(1):299–316. https://doi.org/10.1137/11084008X.
18. Li S, Wang X, Li X, Wu K. Relaxation Oscillations for Leslie-Type Predator–Prey Model with Holling Type I Response Functional Function. Appl Math Lett. 2021;120:107328. https://doi.org/10.1016/j.aml.2021.107328.
19. Lu X, Huang Q. Analysis of Optimal Harvesting of a Predator-Prey Model with Holling Type IV Functional Response. Ecol Complex. 2020;42:100816. https://doi.org/10.1016/j.ecocom.2020.100816.
20. Wei Y, Huo L, He H. Research on Rumor-Spreading Model with Holling Type III Functional Response. Mathematics. 2022;10(4):632. https://doi.org/10.3390/math10040632.
21. Bahlool DK. The Dynamics of a Stage-Structure Prey-Predator Model with Hunting Cooperation and Anti-Predator Behavior. Commun Math Biol Neurosci. 2023;2023:1–23. https://doi.org/10.28919/cmbn/8003.
22. Song Y, Xiao W, Qi X. Stability and Hopf Bifurcation of a Predator–Prey Model with Stage Structure and Time Delay for the Prey. Nonlinear Dyn. 2015;83:1409–1418. https://doi.org/10.1007/s11071-015-2413-6.
23. Li Y, Lv Z, Fan X. Bifurcations of a Diffusive Predator–Prey Model with Prey-Stage Structure and Prey-Taxis. Math Methods Appl Sci. 2023;46(18):18592–18604. https://doi.org/10.1002/mma.9581.
24. Creel S, Christianson D. Relationships Between Direct Predation and Risk Effects. Trends Ecol Evol. 2008;23(4):194–201. https://doi.org/10.1016/j.tree.2007.12.004.
25. Ibrahim HA, Naji RK. Chaos in Beddington–DeAngelis Food Chain Model with Fear. The Fifth International Scientific Conference of Al-Khwarizmi Society (FISCAS), 26-27 June 2020, Iraq. J Phys Conf Ser. 2020;1591:012082. https://doi.org/10.1088/1742-6596/1591/1/012082.
26. Sarkar K, Khajanchi S. Impact of Fear Effect on the Growth of Prey in a Predator-Prey Interaction Model. Ecol Complex. 2020;42:100826. https://doi.org/10.1016/j.ecocom.2020.100826.
27. Mukherjee D. The Effect of Refuge and Immigration in a Predator-Prey System in the Presence of a Competitor for the Prey. Nonlinear Anal Real World Appl. 2016;31:277–287. https://doi.org/10.1016/j.nonrwa.2016.02.004.
28. McNair JN. The Effects of Refuges on Predator-Prey Interactions: a Reconsideration. Theor Popul Biol. 1986;29(1):38–63. https://doi.org/10.1016/0040-5809(86)90004-3.
29. Jabr EAA, Bahlool DK. The Dynamics of a Food Web System: Role of a Prey Refuge Depending on Both Species. Iraqi J Sci. 2021;62(2):639–657. https://doi.org/10.24996/ijs.2021.62.2.29.
30. Majeed SJ, Ghafel SF. Stability Analysis of a Prey-Predator Model with Prey Refuge and Fear of Adult Predator. Iraqi J Sci. 2022;63(10):4374–4387. https://doi.org/10.24996/ijs.2022.63.10.24.
31. Haque Md M, Sarwardi S. Dynamics of a Harvested Prey–Predator Model with Prey Refuge Dependent on Both Species. Int J Bifurcat Chaos. 2018;28(12):1–16. http://dx.doi.org/10.1142/S0218127418300409.
32. Jana S, Guria S, Das U, Kar TK, Ghorai A. Effect of Harvesting and Infection on Predator in a Prey–Predator System. Nonlinear Dyn. 2015;81:917–930. https://doi.org/10.1007/s11071-015-2040-2.
33. Lial ML, Hornsby J, Schneider DI. Precalculus. 3rd edition. USA: Addison-Wesley Educational Publishers Inc. 2004:1176.
34. Murray JD. Mathematical Biology. 1st edition. Berlin: Springer. 1989;770 http://dx.doi.org/10.1007/978-3-662-08539-4.
35. Freedman HI, Waltman P. Persistence in Models of Three Interaction Predator-Prey Populations. Math Biosci. 1984;68(2):213–231. https://doi.org/10.1016/0025-5564(84)90032-4.
36. Perko L. Differential Equations and Dynamical Systems. 3rd edition. USA: Springer. 2001;571 p.

دور الخوف والملجأ المعتمد على المفترس في نظام الفريسة والمفترس ذات المراحل العمرية

غيث جاسم عبدالساده ، هبة عبدالله ابراهيم

قسم الرياضيات، كلية العلوم، جامعة بغداد، بغداد، العراق.

الخلاصة

تناول هذا البحث دور الخوف والملجأ المعتمد على المفترس في نظام الفريسة المفترسة. حيث يصف النظام التفاعل بين الفريسة والمفترس ذي المراحل العمرية مع دالة استجابة وظيفية من النوع هولنك الثاني. حيث ينقسم المفترس إلى قسمين غير ناضج (حدث) وناضج (بالغ). يمكن للحيوانات المفترسة الناضجة أن تكون قادرة على الصيد والتكاثر ولكن هذه القدرة لا توجد في الحيوانات المفترسة غير الناضجة، كما تعتمد الحيوانات المفترسة غير الناضجة على والديها. يتناقص معدل نمو الفرائس بسبب وجود الحيوانات المفترسة الناضجة. يتم التحقق في وجود وتفرد وحدود حل النظام. وتم تحديد ثلاث نقاط توازن للنظام. تم دراسة الاستقرار المحلي للنظام. تمت مناقشة الاستقرار العالمي لنقطة التوازن المحورية باستخدام دالة ليابونوف مناسبة، في حين تم دراسة حوض الجذب لنقطة التوازن الإيجابية. كما وتم تحديد قيود استمرار النظام. تمت دراسة التشعب المحلي وتشعب هوبف للنظام. وأخيرا، تم إجراء عمليات المحاكاة العددية للتأكد من النتائج النظرية بأستخدام برنامج الماتلاب (الاصدار R2018b). وقد وجد أن تأثير الخوف يلعب دورا كبيرا في ديناميكية النظام. ومن ناحية اخرى، فأن معامل الملجأ يؤثر بشكل مستمر على النظام. علاوة على ذلك فأن اختلاف معامل الملجأ مع اختلاف النقاط الاولية يؤدي إلى تغير في سلوك النظام من المستقر إلى غيرالمستقر والعكس.

الكلمات المفتاحية: الحدود، نقاط الاتزان، التشعب المحلي، قيود الثبات، تحليل الاستقرار.